Banerjee et al. reported on the proliferation and differentiation of rat neural stem cells (NSCs) encapsulated within 3-D scaffolds of alginate hydrogels with elastic moduli ranging from 0.18 to 20 kPa created by modulating the concentration of alginate and calcium ions.[77] The rate of NSC proliferation decreased with increases in the hydrogel elastic modulus in expansion medium without added induction factors. Enhanced expression of the neuronal marker β-tubulin III was found within the softest hydrogels, which had elastic moduli comparable to that of brain tissue (approximately 180 Pa).[77] It was found that NSCs cultured on soft substrates were guided to differentiate into neuronal lineages in 3-D[77] and 2-D cultures.[62]

Engler et al. have shown that cytoskeletal motors may be involved in the matrix-elasticity sensing that drives lineage specification in MSCs grown on hydrogels.[32] It is interesting to probe for a possible role for cytoskeletal motors in influencing the function of NSCs in 3-D environments.

Few in vitro studies describe the effects of cell culture matrix elasticity on the differentiation of MSCs into vascular cell types.[37,70,121,122] Wingate et al. fabricated a 3-D PEG-based nanofiber hydrogel coated with collagen type I with tunable elasticity for use as a cellular substrate directing rat MSCs into vascular cell types. This hydrogel is prepared using electrospinning and photopolymerization techniques, and its elasticity is tuned by adjusting the photopolymerization time.[70] The elastic moduli of the hydrogels were determined by compression evaluation to be in the range of 2 to 15 kPa, similar to the in vivo elasticity of the intima basement membrane and media layer where endothelial cells are known to reside on top of the soft basement membrane and smooth muscle cells in the stiffer medial layer.[123,124] MSCs seeded on rigid matrices (8−15 kPa) exhibited an increase in cell area compared with those seeded on soft matrices (2−5 kPa).[70] It was found that the matrix elasticity guided the cells to express different vascular-specific phenotypes with high differentiation efficiency. Ninety-five percent of MSCs cultured on hydrogels with an elasticity of 3 kPa expressed Flk-1 (endothelial marker) protein within 24 h in expansion medium, whereas only 20% of MSCs seeded on matrices with elasticities >8 kPa expressed the Flk-1 marker.[70] In contrast, approximately 80% of MSCs cultured on hydrogels with elasticities >8 kPa expressed α-actin (smooth muscle marker) protein within 24 h in expansion medium, while fewer than 10% of MSCs seeded on hydrogels with elasticities <5 kPa expressed the α-actin marker.[70] In summary, the local elasticity of hydrogels encapsulating MSCs can guide MSC differentiation lineages into vascular cell types in expansion medium without the addition of induction factors, and the lineage commitment of MSCs toward specific vascular cell types can be controlled by the specific design of the substrate modulus.

Mechanical forces are also critical to embryogenesis in the lineage specification of the gastrulation phase, where the embryo is transformed from a spherical cell to a multilayered organism with properly organized endoderm, mesoderm, and ectoderm germ layers. Zoldan et al. investigated the germ layer formation process by culturing hESCs on 3-D scaffolds with stiffnesses corresponding to specific germ layers to understand the environmentally induced cell changes of the embryo in the gastrulation phase.[102] The materials of the scaffolds used in their study were poly(L-lactic acid) (PLLA), poly(lactic acid-*co*-glyconic acid) (PLGA), poly(ε-caprolactone) (PCL), and PEG. The scaffolds were prepared using the salt-leaching method.[3] Binary PLLA/PLGA and ternary PLLA/PLGA/PCL scaffolds were also prepared with selected weight ratios of these biodegradable polymers. The elastic moduli of these scaffolds ranged from 0.05 to 7 MPa. Human ESCs were mixed with Matrigel solution and seeded into the scaffolds to facilitate cell attachment.[102]

Human ESCs cultured on the stiffest scaffolds (>6 MPa) remained undifferentiated and exhibited reduced expression of the germ layer-specific genes evaluated in their study.[102] In contrast, scaffolds with medium-high elastic moduli promoted mesodermal differentiation, and endoderm- and ectoderm-associated gene expressions were not detected.[102] Scaffolds with intermediate elastic moduli (0.1−1 MPa) promoted endoderm differentiation and reduced expression levels of mesoderm-related genes (Brachyury and MIXL1). Scaffolds with low elastic moduli (<0.1 MPa) resulted in ectoderm differentiation, as evidenced by high expression levels of SOX1 and ZIC1 genes (ectodermal germ layer-associated genes).[102] In summary, the differentiation of hESCs into each germ layer was promoted by different scaffold stiffness thresholds, reminiscent of the forces exerted during the gastrulation process. It is possible that 3-D scaffolds could recapitulate the mechanical stimuli required for directing hESC differentiation, depending on the stiffness (elasticity) of the scaffolds.

The liver is one of the most complex organs in the body and is responsible for toxin removal, production of bile and hormones, regulation of nutrients, and synthesis of serum proteins.[65] Hepatic stem cells are partnered in vivo with mesenchymal precursors to endothelia (angioblasts) and stellate cells and reside in regulated microenvironments containing hyaluronic acid (HyA), laminin-5, collagen type III, and chondroitin sulfate proteoglycans. Lozoya et al. investigated the effects of 3-D-microenvironments on human hepatic stem cells by embedding them in HyA-based hydrogels prepared with a serum-free medium tailored for endodermal stem/progenitor cells by mimicking the liver's stem cell niche.[65] These HyA-based hydrogels matched the diffusivity of culture medium and had tunable stiffness (25−520 Pa), depending on their concentration of HyA and cross-linker (poly(ethylene glycol) diacrylate). The HyA-based hydrogels induced the transition of hepatic stem cell colonies toward stable heterogeneous populations of hepatic progenitors (hepatoblasts) depending on hydrogel stiffness, as shown by both their gene and protein expression profiles.[65] This study shows that the mechanical properties of the microenvironment can regulate differentiation in endodermal stem cell populations, such as human hepatic stem cells.

2.5. Results Contradictory to Engler's Research in 2-D Culture

Although Engler et al.[32] performed the landmark study, demonstrating that substrate matrix guides stem cell differentiation fate (1850 citation by Web of Science in September, 2012), the mechanism by which stem cells sense the mechanical and geometrical properties of the substrate has remained elusive.[125] Several researchers have reported conflicting results and different intriguing ideas on the effect of substrate elasticity on stem cell differentiation.[19,22]

Trappmann et al. investigated the differentiation of hMSCs and human epidermal stem cells on (a) polydimethylsiloxane (PDMS) with immobilized collagen type I and (b) PAAm hydrogels with immobilized collagen type I.[22] PDMS and PAAm substrates of varying stiffness in the range of 0.1 kPa to

2.3 MPa were prepared by varying the ratio of cross-linker to base monomers. They found that epidermal stem cells could spread fully and assemble a cortical F-actin cytoskeleton on all PDMS substrates, independent of stiffness. Furthermore, cells cultured on all PDMS substrates reached terminal epidermal stem cell differentiation (i.e., keratinocytes) and expressed the cornified envelope precursor involucrin at the same rate (i.e., approximately 25%). Thus, PDMS elasticity (stiffness) did not affect the differentiation or spreading of human epidermal stem cells.[22] Furthermore, osteoblast differentiation, as analyzed by alkaline phosphatase (Table 3), was observed to the same degree (approximately 35%) on PDMS substrates of varying stiffness in the range of 0.1−800 kPa. No effect of PDMS substrate stiffness on the differentiation of hMSCs into osteoblasts was observed. Adipogenic differentiation of hMSCs as analyzed by Oil Red O staining (Table 3) was also investigated on PDMS substrates of varying stiffness. As was found in osteogenic differentiation on PDMS substrates, no effect of PDMS substrate stiffness was noted on the differentiation of hMSCs into adipocytes. These results can be explained by the fact that the morphology and characteristics of the ECM (collagen I in this case) should be almost the same on PDMS substrates of different elasticities because ECM cannot penetrate the surface of PDMS substrates, whereas it can penetrate the surface of hydrogels, as depicted in Figure 9.

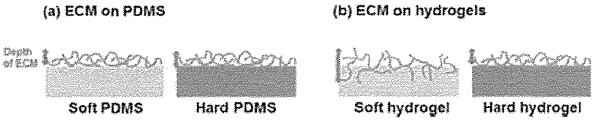

Figure 9. Morphology of ECM on PDMS (a) and hydrogel (b) with soft and hard characteristics.

Other researchers have also reported no effects of PDMS substrate stiffness on the differentiation of hMSCs.[85]

In contrast, adhesive cell area and actin polymerization of hMSCs cultured on PAAm hydrogels grafted with collagen type I increased with increasing elastic modulus of the PAAm hydrogels, the same tendency reported by several researchers in 2-D culture of hMSCs on PAAm hydrogels coated with collagen type I.[32] In summary, the differentiation of hMSCs is influenced by the stiffness of PAAm but not PDMS substrates.[22]

Stiffer PAAm hydrogels have higher cross-linking points. Therefore, differences in PAAm hydrogel network cross-linking will result in differences in collagen attachment, with the distance between covalent anchoring points being longer on softer gels, whereas anchoring point distance is shorter on stiffer gels, as described in Figure 9. ECM can anchor into stiffer hydrogels with higher anchoring points, whereas ECM can anchor into softer hydrogels with lower anchoring points. In our recent study, it was found via XPS ECM analysis that ECM concentration on the outer surface is higher on stiffer hydrogels and lower on softer hydrogels, whereas the total ECM amount on the hydrogels was found to be nearly unchanged using measurements of fluorescent probe binding to the ECM (unpublished data), as reported in several previous studies.[32,74] Therefore, the depth of ECM anchoring is expected to be deeper on softer hydrogels, as depicted in Figure 9. The ECM anchoring depth may be another factor regulating stem cell differentiation lineage fate.

When cells pull on covalently attached collagen, the mechanical feedback consists of the magnitude of the movement of the collagen segment coupled to the PAAm hydrogel. Therefore, the strength of the collagen elasticity feedback that cells sense upon integrin ligation decreases with increasing anchored collagen fiber length (i.e., on soft PAAm hydrogels).[22,125] In contrast, collagen stiffness on PDMS substrates of varying stiffness is suggested to be the same due to the same collagen cross-linking time leading to the same collagen cross-linking distance. This may be because collagen cannot penetrate into PDMS substrates of any stiffness.

Rowlands et al. demonstrated the interplay of stiffness and adhesive ligand presentation, exemplified by the observation that osteogenic differentiation of hMSCs occurred significantly only on collagen type I-coated substrates with the highest tested substrate stiffness.[88] The modulation of osteogenic and myogenic transcription factors by various ECM proteins demonstrated that substrate stiffness alone did not direct stem cell lineage specification, but the combination of substrate stiffness and specific ECMs, that is, the stiffness of specific ECMs, seemed to direct stem cell fate into specific differentiation lineages in 2-D culture.

It is concluded that Engler's landmark study demonstrating that substrate matrix guides stem cell differentiation fate is verified under the limited condition that the stem cells are cultured on hydrogels with immobilized collagen type I in a 2-D system where ECM (e.g., collagen type I) can penetrate the hydrogel surface to some extent, and not on solid substrates where ECM cannot penetrate the substrate surface, such as PDMS, glass, or metal. Hydrogels of varying stiffness lead to differences in ECM anchoring densities, thereby altering the mechanical feedback of ECM on stem cells. When the ECM is more loosely bound on soft hydrogels, we think that it cannot provide the mechanical feedback that the integrin complex requires to cluster in focal adhesions and signal through ERK/MAPK. It seems that mechanical feedback in stem cells leads them into specific differentiation lineages or causes them to remain undifferentiated.

2.6. Results Contradictory to Engler's Research in 3-D Culture

As discussed in previous sections, stem cells sense and respond to mechanical properties of the ECM. However, how ECM mechanics biophysically affect stem-cell fate in 3-D microenvironments is difficult to determine. Huebsch et al. demonstrated that the lineage commitment of murine MSCs changed in response to the rigidity of 3-D microenvironments. The highest osteogenesis of MSCs was predominantly generated in alginate gels grafted with RGD oligopeptide (RGD-modified alginate) at 11−30 kPa, whereas MSCs preferentially differentiated into the adipogenic lineage in softer alginate gels (2.5−5 kPa).[19] The tendency for substrate stiffness to affect MSC differentiation lineage was also observed in various types of hydrogels, i.e., RGD-modified agarose and RGD-modified PEG hydrogels, and RGD-modified alginate.[19] The relationship between stem cell morphology and differentiation direction in 3-D hydrogels was investigated because hydrogel matrix elasticity affects stem cell morphology in 2-D culture, which correlates with MSC differentiation fate. However, the elastic modulus had no significant influence on MSC morphology in the 3-D hydrogels.[19] In other words, in the 3-D hydrogels, stem cell fate was not correlated with cell morphology, in contrast to previous 2-D work.[32] Instead, matrix

stiffness regulated integrin binding and the nanoscale reorganization of adhesion ligands, both of which were traction dependent and correlated with MSC osteogenic commitment.[19] It seemed that the stem cells used traction forces to mechanically reorganize the RGD peptides presented by the hydrogel matrices on a nanometer scale, clustering RGD near integrins while the peptides remained bound to the hydrogel material (Figure 10).[19] It was found that RGD clustering was

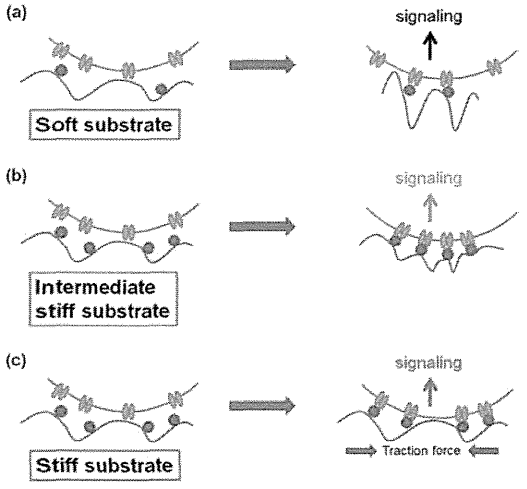

Figure 10. Matrix stiffness (soft substrate [a], intermediate substrate [b], and stiff substrate [c]) regulates integrin binding and reorganization of adhesion ligands, which are traction-dependent, at the nanometer level.

maximized in hydrogels of intermediate rigidity (22 kPa). This can be explained by the fact that stem cells in extremely soft hydrogels cannot assemble the cytoskeleton-associated adhesion complexes required to exert traction force, preventing them from deforming the hydrogel matrix to generate RGD clustering and maintain the RGD–integrin complex.[19] Blocking RGD–integrin binding to α_5 and α_V integrins by using anti-α_5- or anti-α_V-antibodies significantly decreased osteogenesis in RGD-modified alginate in 3-D culture and enhanced adipogenesis in an antibody dose-dependent fashion. In contrast, only α_5 integrins were expressed on the surfaces of MSCs in 2-D culture and were used to differentiate into osteoblasts.[19]

It is possible that MSCs interpret changes in the physical properties of adhesion substrates as changes in adhesion-ligand presentation and that MSCs themselves can be harnessed as tools to mechanically process materials into structures that feed back to manipulate their fate.

3. EFFECT OF TOPOGRAPHY OF CELL CULTURE MATERIALS ON STEM CELL DIFFERENTIATION

The topography of the extracellular microenvironment can influence stem cell responses from attachment and migration to differentiation and production of new tissues.[126−129] Cells in their natural environment interact with ECM components on a nanometer scale.[130] There is evidence of nano- or macro-topography-induced stem cell differentiation, suggesting that physical interactions between stem cells and the extracellular environment in the form of topography can modulate cell function and stem cell differentiation.[60] The regulation of cell spreading area and shape in 2-D culture is one of the physical factors affecting stem cell differentiation fate that can be guided by the topography of cell culture biomaterials (substrates). Micro- and nanopatterned surfaces with and without immobilized ECM are one of the most typical cell culture biomaterials used for topography regulation. In this section, we will discuss the effect of biomaterial topography on stem cell differentiation on micro- and nanopatterned surfaces.

3.1. Preparation of Micro- and Nanopatterned Surfaces

Micro- and nanopatterned surfaces are the most common biomaterials used to investigate the effect of cell culture topography on stem cell differentiation. Microcontact printing (soft lithography) and photolithography patterning (hard lithography) methods are typically used to create micro- and nanopatterned surfaces. A variety of shapes, morphologies, sizes, and microdomain stem cell attachment patterns can be designed using both of these methods.

Some examples of the shapes and morphologies of micro- and nanodomains of micropatterned surfaces are illustrated in

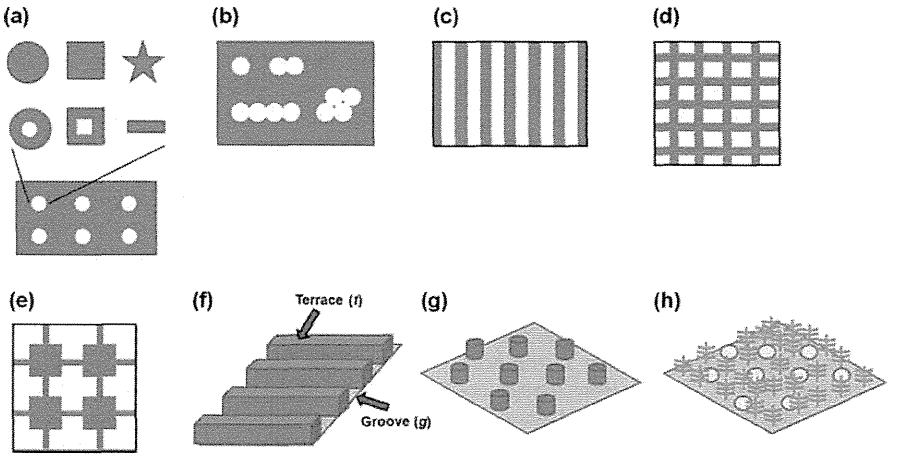

Figure 11. Examples of shapes and morphologies of micropatterned surfaces reported in the literature. Circles, squares, and stars (a), circle combinations (b), stripes (c), grids (d), grid and square combinations (e), microgroove morphologies (f), microposts (g), and circles surrounded by polymer brushes (h) are illustrated.

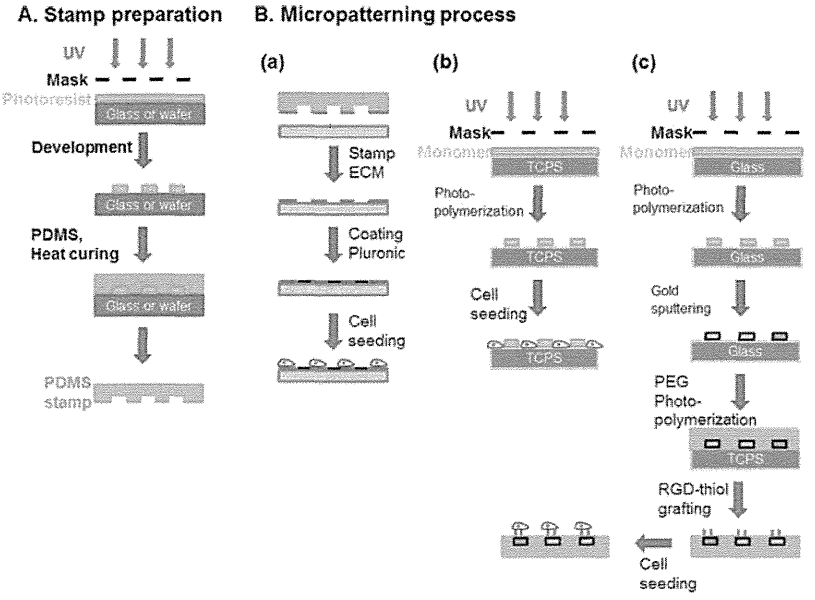

Figure 12. Typical microcontact printing preparation methods in two-dimensional (2-D) stem cell culture. Stamp preparation method (a) and several micropatterning processes (b).

Figure 11. Circles, squares, stars, striped lines, and grid lines are typically used as stem cell attachment macro-domains (Figure 11a,b,c,d).[131−133] Surface patterns of squares connected with narrow lines have also been investigated (Figure 11e).[134] Striped and microgrooved surface morphologies have been investigated for stem cell culture (Figure 11f).[135] Patterned cylinder (micropost) (Figure 11g),[136] and cave (Figure 11h)[137−139] structures have also been prepared.

A typical preparation method of microcontact printing for the 2-D culture of stem cells is illustrated in Figure 12. First, a polydimethylsiloxane (PDMS) elastomeric stamp is prepared using a mold. The mold can be fabricated by spin-coating a photoresist solution onto silicon wafers or glass cover plates and then exposing the photoresist to ultraviolet (UV) light through a chrome mask with the desired geometric features (Figure 12A).[131] Un-cross-linked polymer (photoresist) is removed by washing the silicon wafer or glass cover plates with solvent. PDMS and curing agent prepolymers are poured on the resulting mold and cured at a high temperature (i.e., 70 °C) for several hours before the PDMS stamp is removed from the mold.[131] ECM solutions such as fibronectin,[95,131,140] Matrigel,[141−143] collagen type I, laminin, or poly(L-lysine) (PLL) solution[134] are stamped on PDMS films,[95,140] Petri dishes,[134] TCPS dishes or slides,[141−143] and glass slides. Although stem cells specifically adhere to ECM or PLL domains, nonspecific adsorption outside the microcontact patterning domains on PDMS films, TCPS dishes or slides, or glass slides should be avoided. Because stem cells are adhered to the biomaterial surface via proteins such as ECM, low-protein-binding macromolecules, such as a triblock copolymer of poly(ethylene oxide) (PEO)−poly(propylene oxide) (PPO)−poly(ethylene oxide) (PEO), Pluronic or Poloxamer,[144−146] are typically coated on micropatterned dishes and slides after stamping with ECM or PLL. In other cases, ECM or PLL is stamped on Petri dishes coated with plasma-polymerized PEO using a PDMS microstamp in which PEO is one of the low-protein-binding polymers.[134] Microprinting is a simple way to prepare micropatterned surfaces; however, the drawback of microprinting ECMs or PLL is the low stability of the remaining micropatterned ECM or PLL on the surface due to their physical adsorption.

The self-assembly monolayer (SAM) method can be combined with microcontact printing. Wan et al. prepared micropatterned fibronectin using the SAM method.[131] An adhesive SAM octadecanethiol was transferred via PDMS microstamp onto gold-coated glass slides. Subsequently, the unstamped regions of the slides were coated with nonadhesive ethylene glycol-terminated SAM. Finally, the patterned surfaces were coated with fibronectin solution because fibronectin preferentially adsorbed on the hydrophobic domain of SAM octadecanethiol in the microcontacted region.[131]

Hydrogels such as poly(vinyl alcohol) (PVA) and PEO or PEG display low protein-binding activity. Chen et al. developed an interesting and simple micropatterning method (Figure 12B,b).[137,139] They synthesized photo-cross-linkable azidophenyl-derived PVA.[137,139] The photo-cross-linkable PVA solution was placed on TCPS and cross-linked via a micropatterned photomask. The PVA was cross-linked and used to generate hydrogels on the outside of stem cell culture domains. This allowed stem cells to be cultured on micropatterned TCPS surrounded by cross-linked hydrogels. If necessary, ECM can be coated on the micropatterned TCPS dishes. A similar strategy using a different method was reported by Connelly et al.[138] Micropatterned stamps inked with the thiol initiator ω-mercaptoundecyl bromoisobutyrate were brought into conformal contact with gold-coated coverslips to deposit the initiator as a self-assembled monolayer.[138] Atom transfer radical polymerization (ATRP) of oligo(ethylene glycol) methacrylate (OEGMA) was performed on the gold-coated coverslips. Finally, the micropatterned coverslips were coated with collagen type I, which could be loaded on the regions without micropatterned OEGMA polymer brush. Stem cells were cultured on bowls surrounded by hydrogel polymers on micropatterned dishes prepared from either PVA or

Table 6. Some Research Studies for Stem Cell Differentiation on Micropatterned Materials (Osteogenic and Adipogenic Differentiation)[a]

stem cell source	micropatterned materials for stem cell culture	pattern type	medium	differentiation	ref (year)
hMSCs	micropatterned amorphous diamond, titanium, tantalum, and chromium with square shape on silicon wafer	Figure 11a	differentiation medium	osteoblasts	147 (2010)
murine MSCs	micropatterned PDMS with grid (lattice) morphology coated with fibronectin	Figure 11d	differentiation medium	osteoblasts	151 (2011)
hADSCs	micropatterned fibronectin with ring shape or rectangles on gold-coated slides	Figure 11a	differentiation medium	osteoblasts, adipocytes	131 (2010)
hMSCs	micropatterned fibronectin with square, rectangular, flower, and star shape on octadecanethiol surface	Figure 11a	mixed differentiation media of adipocytes and osteoblasts	adipocytes, osteoblasts	79 (2010)
hMSCs	micropatterned fibronectin with square shape on PDMS surrounded by Pluronic F108	Figure 11a	mixed or single differentiation medium of adipocytes and osteoblasts	adipocytes, osteoblasts	95 (2004)
rat MSCs	micropatterned RGD with circle, square, triangle, and star shape on PEG hydrogel	Figure 11a	differentiation medium	adipocytes, osteoblasts	148 (2011)
hMSCs	micropatterned alkane thiol surface with circle, octagone, triangle, trapezoid, square, and pentagone shape surrounded by PEG-terminated alkanethiol on gold surface	Figure 11a	differentiation medium	adipocytes	137 (2008)
rat MSCs	micropatterned RGD with circle and aggregated circle shape on PEG hydrogel	Figure 11b	differentiation medium	adipocytes, osteoblasts	132 (2010)
hMSCs	TCPS surface of circle shape surrounded by micropatterned poly(vinyl alcohol)	Figure 11h	differentiation medium	adipocytes, osteoblasts	139 (2011)
hMSCs	TCPS surface of triangle, square, pentagon, hexagon, and circle shape surrounded by micropatterned poly(vinyl alcohol)	Figure 11h	differentiation medium	adipocytes	149 (2011)

[a]hADSCs, human adipose-derived stem cells; MSCs, mesenchymal stem cells; hMSCs, human MSCs; PDMS, polydimethylsiloxane; TCPS, tissue culture polystyrene.

OEGMA polymer brushes, making it possible to restrict the stem cells from leaving the bowl where they were intended to stay (Figure 11h).

Tang et al. developed a slightly different preparation method of the micropatterned surfaces described above (Figure 12B,c).[132] Clean glass slides were spin-coated with a positive photoresist, exposed to UV light through a chrome mask with the desired geometric features, and developed. Subsequently, the surface was sputtered with gold, and the unpolymerized photoresist was removed by washing with solvent. Allylmercaptan was grafted on the gold microislands in a vacuum. This process was necessary to transfer the gold onto the surface of the PEG hydrogel in the following step. PEG diacrylate with a photoinitiator was cast onto the micropatterned glass and photo-cross-linked under UV irradiation. Micropatterned PEG hydrogel was finally obtained by separating the hydrogel bound with the gold micropatterns from the glass slides. Cyclo-(RGDfk)-thiol (R, arginine; G, glycine; D, aspartic acid; f, D-phenylalanine; and k, lysine) was grafted onto the gold microislands on the PEG hydrogels. Stem cells were able to attach to the RGD microdomain on the PEG hydrogels via integrin receptors.

Microgrooved surfaces with striped terraces and grooves (Figure 11f) can be prepared using conventional photolithographic techniques. Beduer et al. prepared microgrooved surfaces on PDMS, and PLL and laminin were then coated on the microgrooved surface for neural stem cell culture.[135]

3.2. Adipogenic and Osteogenic Stem Cell Differentiation on Micropatterned Surfaces

Evidence that cell shape regulation by micropatterned surfaces leads to the commitment of stem cells into different lineages has been identified in 2-D cultures. Several researchers have investigated the effect of the spreading area and shape of stem cells cultured on micropatterned surfaces on differentiation lineage commitment.[67,79,95,131,133,135,139,147−150] Table 6 summarizes a number of studies of stem cell differentiation into adipocytes and osteoblasts on micropatterned surfaces.[79,95,131,132,137,139,147−149,151]

It is known that cell seeding density directly affects hMSC lineage commitment; hMSCs at high seeding density tend to differentiate into adipocytes, and those at low seeding density tend to differentiate into osteoblasts when cultured in mixed differentiation medium for osteoblasts and adipocytes (Figure 13d).[95] These phenomena can be explained by (a) a decrease in cell adhesion and spreading on the cell culture substrate or (b) an increase in cell−cell contact and paracrine signaling. However, conventional cell culture cannot distinguish between these two potential effects. Therefore, McBeath et al. investigated the effect of cell shape on stem cell differentiation commitment by controlling the degree of cell spreading in the absence of cell−cell communication.[95] They placed square shaped microcontact fibronectin prints onto PDMS substrates to generate "islands" of fibronectin surrounded by regions coated with Pluronic F108, which enables stem cells to adhere on fibronectin islands (Figure 11a).[95] Human MSCs were seeded on the micropatterned PDMS substrates by attaching as single cells per island and spread to varying degrees, depending on the size of the island (1000 or 10 000 μm^2) in mixed differentiation medium for adipocytes and osteoblasts. Adipogenesis occurred only on small islands, indicating that round hMSC morphology guided their differentiation commitment into adipogenesis, whereas osteogenesis was observed only on large islands, suggesting that hMSC spreading led to osteogenic differentiation (Figure 13a). In their results, it is suggested that the regulation of cell shape alone can mediate a switch in hMSC commitment between adipogenic and osteogenic fates in 2-D culture.[95] Shape-mediated commitment was facilitated by actin-cytoskeleton expression because disrupting the actin cytoskeleton by the addition of the actin-disrupting agent cytochalasin D or the Rho kinase inhibitor (ROCK) Y-27632 into the mixed differentiation medium increased adipogenesis and decreased osteogenesis of hMSCs in both cases of inhibitor addition where the Rho effector was involved in myosin

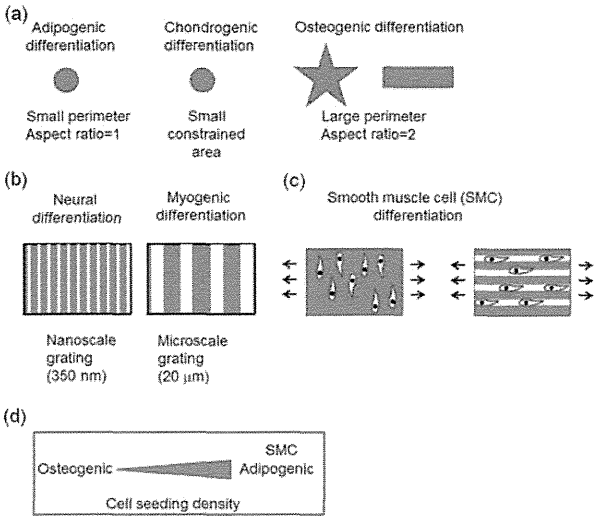

Figure 13. Stem cell differentiation on several different micropatterned surfaces. Adipogenic stem cell differentiation is promoted on surfaces with smaller perimeters and lower aspect ratios. Chondrogenic stem cell differentiation is promoted on surfaces of constrained area. Osteogenic stem cell differentiation is promoted on surfaces with larger perimeters and relatively high aspect ratios (a). Surfaces with nanoscale grating promote neural stem cell differentiation, whereas surfaces with microscale grating promote myogenic stem cell differentiation (b). Micropatterned surfaces with striped groove (grating) morphologies promote stem cell differentiation into smooth muscle under uniaxial strain (c). Lower cell seeding density promotes osteogenic stem cell differentiation, whereas higher cell seeding density promotes the differentiation of stem cells into smooth muscle cells or adipocytes (d).

activation. The commitment switch between adipocyte and osteoblast was suggested to be mediated through the RhoA–ROCK signaling pathway; cell shape regulation and RhoA activity were both necessary, but neither was sufficient, to drive the switch in hMSC commitment.[95]

Cell shape can be regulated by the shape of the adhesion domain on the micropatterned surface. Therefore, Kilian et al. precisely investigated the effect of adhesive area, aspect ratio, and subcellular curvature of micropatterned surfaces on adipocyte and osteoblast hMSC commitment. Human MSCs were cultured on micropatterned fibronectin islands with rectangular, star, and flower shapes on glass plates at varying aspect ratios and curvatures in mixed differentiation medium for adipocytes and osteoblasts. The aspect ratio was defined as the ratio of the width of the fibronectin shape at its long axis to its width at its short axis (Figure 11a).[79] When hMSCs were cultured on small islands (e.g., 1000 μm^2) of varying shapes, most of the cells differentiated into adipocytes in the mixed differentiation medium (Figure 13a). In contrast, hMSCs differentiated into osteoblasts when they were cultured on large islands (e.g., 5000 μm^2). These results indicate that the size of the cell adhesion area predominantly guides stem cell differentiation fate, as in McBeath's results.[95] Human MSCs cultured on several patterns of intermediate area (2500 μm^2) differentiated into a mixed population of adipocytes and osteoblasts. Therefore, the effect of shape, aspect ratio, and curvature of the cell adhesion domain on hMSC differentiation commitment was investigated at a constant cell adhesion area of 2500 μm^2 in mixed differentiation media.[79]

Human MSCs cultured on rectangular islands with aspect ratios of 1:1, 3:2, and 4:1 demonstrated that osteogenesis increased with aspect ratio (Figure 13a). Human MSCs cultured in rectangles with aspect ratios of 4:1 were 61% osteogenic, while hMSCs cultured in squares (aspect ratio 1:1) were only 46% osteogenic.[79] Human MSC cultivation on flower-shaped islands with large convex curves along each edge displayed 62% adipogenic differentiation, while hMSCs cultured on star-shaped islands with concave edges and sharp points at the vertices displayed 62% osteogenic differentiation. Human MSCs cultured on pentagon-shaped islands with straight lines for the edges were evenly differentiated into both adipocytes and osteoblasts.[79,137,148] These experiments are striking in that the subtle geometric differences of stem cell adhesion domains are significantly important in directing stem cell differentiation lineage commitment in 2-D culture. It has been suggested that the stem cell shape alone can influence the direction of their differentiation in 2-D culture.[79,137] Stem cell shape is organized by cytoskeleton components, such as stress fibers and focal adhesion complexes. Human MSCs cultured on the star-shaped islands exhibited larger focal adhesions and stress fibers than those cultured in flower shapes. Furthermore, a higher degree of actomyosin contractility along the edges was observed in immunofluorescent staining images of myosin IIa in hMSCs cultured in star shapes.[79] It may be that local curvatures of stem cell shapes that increase cytoskeletal tension and contractile stem cell cytoskeletons promote osteogenesis relative to adipogenesis. Microarray analysis and pathway inhibition studies suggest that stem cell contractility promotes osteogenesis by enhancing c-Jun N-terminal kinase (JNK) and extracellular-related kinase (ERK1/2) activation in conjunction with elevated wingless-type (Wnt) signaling (e.g., downstream effectors of RhoA and Rock signaling).[79] The geometric shapes of stem cells cultured on varying adherent shapes play roles in orchestrating mechanochemical signals and paracrine/autocrine factors that can direct hMSCs to appropriate differentiation lineage fates.

Chen et al. investigated whether differing geometries with small surface areas (e.g., 1100 μm^2) have an effect on the adipogenesis of hMSCs in an adipogenic induction medium.[149] In this investigation, micropatterned TCPS surrounded by photo-cross-linked PVA with cell adhesion geometries of triangles, squares, pentagons, hexagons, and circles of fixed surface area was used in a single hMSC culture. The cellular shapes of the hMSCs adopted nearly the same geometries as the micropatterns. Human MSCs cultured on islands with differing micropatterns predominantly assembled actin filaments along the peripheral edges of the micropatterns, indicating that the cells were sensing their peripheral microenvironment.[149] However, hMSCs cultured on nonpatterned TCPS dishes had much stronger actin filaments and stress fibers in their peripheral and central regions. Human MSCs cultured on islands of differing geometries with small surface areas showed similar adipogenic differentiation potentials.[149] However, hMSCs cultured on islands of micropatterned geometries differentiated into adipocytes at significantly higher rates than those cultured on nonpatterned TCPS dishes, consistent with the result reported by several researchers that smaller spreading areas favor adipogenic hMSC differentiation.[79,95]

Wan et al. investigated the expansion and differentiation potentials of human adipose-derived stem cells (hADSCs) on different shapes and sizes of micropatterned surfaces upon

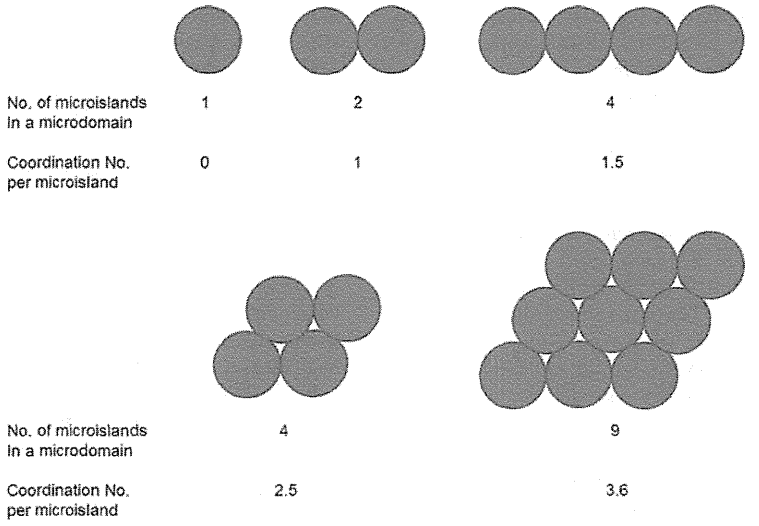

Figure 14. Micropatterned domains consisting of 1−9 microislands with 30 μm diameters. Coordination numbers per island are estimated to be 0, 1, 1.5, 2.5, and 3.6 in microdomains consisting of 1, 2, 4, 4, and 9 microislands, respectively.

Table 7. Some Research Studies for Stem Cell Differentiation on Micropatterned Materials (Cardiomyocyte, Chondrocyte, Smooth Muscle Cell, Neuronal Cell, Epidermal Cell, and Hepatocyte Differentiation)[a]

stem cell source	micropatterned materials for stem cell culture	pattern type	medium	differentiation	ref (year)
hESCs	micropatterned matrigel of circular shape surounded by Pluronic F-127 on TCPS	Figure 11a	differentiation medium	cardiomyocyte	143 (2009)
hMSCs	micropatterned fibronectin with square shape surroundedby Pluronic F127 on PDMS film	Figure 11a	expansion or differentiation medium	smooth muscle cell, chondrocyte	67 (2010)
hESCs	micropatterned matrigel of circular shape surounded by Pluronic F-127 on TCPS	Figure 11a	differentiation medium	mesoderm cells, cardiomyocyte	142 (2008)
hMSCs	microprinting fibronectin with stripe shape on PLGA	Figure 11c	expansion medium	cardiomyocyte	133 (2010)
hMSCs	micropatterned PDMS with striped groove morphology coated with collagen type I	Figure 11f	expansion medium	smooth mucle cells	152 (2006)
iPSCs	micropatterned PDMS with striped groove morphology coated with collagen type I	Figure 11f	differentiation medium	smooth muscle cells, neuronal cells	156 (2011)
mESCs	micropost array made of PDMS coated with fibronectin	Figure 11g	no description	cardiomyocyte	136 (2009)
NSCs	micropatterned PLL with square shape connected with and without line on PEO film	Figure 11a and 11e	differentiation medium	neuronal cells	134 (2008)
hNSCs	micropatterned PDMS with striped groove morphology coated with PLL and laminin	Figure 11f	differentiation medium	neuronal cells	135 (2012)
adult rat hippocampal progenitor cells	micropatterned polystyrene with striped groove morphology coated with PLL, laminin, or both	Figure 11f	differentiation medium	neuronal cells	153 (2006)
hMSCs	micropatterned amorphous carbon with striped groove morphology	Figure 11f	differentiation medium	neuronal cells	154 (2010)
hMSCs	micropatterned PDMS with striped groove morphology coated with collagen type I	Figure 11f	expansion medium	neuronal cells	126 (2007)
human epidermal stem cells	micropatterned collagen-coated circle shape surrounded by grafted PEG on gold-coated coverslips	Figure 11h	differentiation medium	epidermal cells	150 (2011)
mESCs	micropatterned protein (collagen type I, fibronectin, and growth factors) microarray with circle shape on glass slide	Figure 11a	differentiation medium	hepatocytes	155 (2010)

[a]ESCs, embryonic stem cells; hESCs, human ESCs; hMSCs, human MSCs; NSCs, neural stem cells; hNSCs, human NSCs; iPSCs, induced pluripotent stem cells; TCPS, tissue culture polystyrene; PEO, poly(ethylene oxide).

which hADSCs were cultured.[131] The micropatterned surfaces had ring (rings 500 or 1000 μm in diameter and 100 or 200 μm in width) or rectangular structures (500 or 1000 μm long and 100 or 200 μm wide) coated with fibronectin on microprinted SAM octadecanethiol on a gold-coated glass surface.[131] The highest rates of cell proliferation were observed at the outer edge of the ring patterns and along the short axes of the rectangle patterns, where hADSC morphology was large and spreading.[131] Human ADSCs that exhibited high adipocyte and osteoblast differentiation were increased on the inner edges of the ring structures and on regions next to the narrow ends of rectangles, where hADSC morphology was small and elongated. These results can be attributed to the cytoskeletal tension associated with cell shape.[131]

Micropatterned surfaces make it possible to study the effects of stem cell spreading and shape on single-cell differentiation by

dx.doi.org/10.1021/cr300426x | Chem. Rev. 2013, 113, 3297−3328

the culture of a single cell on each patterned island; it is also possible to study the effect of cell−cell contact between stem cells on cell differentiation by controlling cell contact numbers via the design of specific micropatterned surfaces. Tang et al. designed several unique micropatterned domains grafted with RGD on PEG hydrogels as shown in Figure 14.[132] The micropatterned domain was composed of 1−9 microislands 30 μm in diameter, allowing single cells to bind on each microisland circle. The coordination numbers per island were estimated to be 0, 1, 1.5, 2.5, and 3.6 in microdomains consisting of 1, 2, 4, 4, and 9 microislands, respectively, as illustrated in Figure 14.[132] The researchers observed that alkaline phosphatase activity, an early marker of osteogenesis, increased with coordination number. Adipogenic differentiation of rat MSCs, as measured by Oil Red O staining (counting cells with lipid droplets), also increased with coordination number.[132] Inhibiting gap junctions between cells with 18α-glycyrrhetinic acid (AGA) treatment dramatically suppressed adipogenic and osteogenic differentiation of rat MSCs on all microdomains regardless of coordination number.[132] The micropatterned surface enables the study of the effects of cell−cell contacts and gap junctions on stem cell differentiation potential.

The effect of topographical variation on murine MSC osteogenic differentiation has also been reported. Seo et al. prepared micropatterned PDMS with an ordered lattice morphology consisting of a fixed pattern width of 2 μm, a fixed pattern height of 1 μm, and varied pattern intervals of 0, 1, 2, 3, 4, 6, and 8 μm.[151]

When murine MSCs were cultured on the micropatterned PDMS surface coated with fibronectin, gene expression of collagen type I, the major extracellular component of bone, osteocalcin, an osteogenesis marker, and alkaline phosphatase, an early marker of osteogenesis, was found to increase with increased pattern interval up until an interval of 3 μm.[151] However, with pattern intervals greater than 3 μm, gene expression of collagen type I, osteocalcin, and alkaline phosphatase decreased with increasing pattern interval. Therefore, gene expression indicating osteogenic differentiation of MSCs was highest on PDMS surfaces with lattice micropattern morphology pattern intervals of 3 μm.[151] These results demonstrated that the topography of micropatterned substrates is a significantly positive regulator of stem cell osteogenic differentiation in 2-D culture.

3.3. Chondrogenic, Myogenic, and Hepatic Stem Cell Differentiation on Micropatterned Surfaces

Table 7 summarizes a number of research studies regarding stem cell differentiation into chondrocytes, myocytes, hepatocytes, or neural cells on micropatterned surfaces (refs 67, 126, 133−136, 141−143, 150, and 152−156).

Chondrogenic differentiation of hMSCs can be induced in pellet culture mimicking cellular condensation during cartilage development with exposure to transforming growth factor β (TGF-β). TGF-β can also induce hMSC differentiation into smooth muscle cells (SMCs).[67] However, it is unclear which cell culture and environmental parameters can direct commitment between these two lineages. Gao et al. investigated differentiation switching between chondrogenic and SMC fates when hMSCs were cultured on micropatterned square surfaces (1000 μm^2 or 10 000 μm^2 islands) of fibronectin on PDMS substrates prepared with the microprinting method.[67] Human MSCs with well-spread morphologies on large micropatterned islands (10 000 μm^2) upregulated SMC genes with TGF-β stimulation, whereas hMSCs on small micropatterned islands (1000 μm^2) that were prevented from spreading and flattening upregulated chondrogenic genes.[67] hMSCs undergoing SMC differentiation exhibited little change in RhoA but had significantly higher Rac1 activity than chondrogenic differentiated cells. Rac1 activation inhibited chondrogenic hMSC differentiation and was necessary for SMC differentiation, whereas RhoA activity is known to mediate the shape-dependent control of hMSC lineage commitment to osteoblasts or adipocytes.[95] Rac1 signaling also upregulated N-cadherin, which was required for SMC differentiation.[67] In this study, it was demonstrated that hMSC commitment to chondrogenic or SMC lineage is mediated by cell shape, Rac1, and N-cadherin.[67]

Control of hESC differentiation into specific lineages with high efficiency is currently a difficult task. One reason for this is the heterogeneity of hESC colonies, while hESC culture on a micropatterned surface provides size-controlled aggregates of hESCs.[142,143] Niebruegge et al. prepared uniformly sized hESC aggregates by culturing hESCs on circular Matrigel islands 400 or 800 μm in diameter, which were microstamped on TCPS dishes and coated with (i.e., surrounded by) the non-protein-adsorbent Pluronic F127.[143] After 2−3 days, when uniformly sized hESC aggregates were formed, the aggregates were shifted into bioreactors and cultured in cardiac differentiation medium under hypoxia (4% oxygen tension). Under hypoxia, the uniformly sized hESC aggregates could differentiate toward cardiomyocytes with high efficiency.[143] Human ESC aggregates after differentiation were able to spontaneously beat, indicating that uniformly sized differentiated hESC aggregates generated some cardiomyocyte functions.[143]

Mechanical stimulation of blood vessel walls in vivo is considered to play an important role in the differentiation of MSCs into vascular SMCs. Several studies have suggested that mechanical strain enhances differentiation of MSCs and neural crest stem cells into vascular SMCs.[152,156−159] However, MSCs aligned perpendicularly to the axis of strain after long-term stimulation with cyclic uniaxial strain (Figure 13c), causing a decrease in SMC markers after an initial up-regulation. This cellular orientation differs from that observed in in vivo conditions, where vascular SMCs align in the circumferential direction.[152,160,161] To guide stem cells into parallel alignment with the axis of strain, Kurpinski et al. cultured hMSCs for two days on micropatterned PDMS sheets with a striped groove (grating) morphology of 10 μm terrace width, 10 μm groove spacing, and 3 μm depth and on which collagen type I had been coated under uniaxial strain (5%, 1 Hz) (Figure 13c).[152] Increases in contractile markers (e.g., calponin 1) and decreases in chondrogenic/osteogenic ECM markers were observed in hMSCs cultured on the micropatterned PDMS sheets under uniaxial strain.[152] Cartilage matrix proteins were observed to decrease significantly with uniaxial strain, suggesting that tensile stress suppressed the phenotype of compression-bearing tissue.[152] The surface of micropatterned biomaterials can regulate cell alignment direction even under uniaxial strain, thereby guiding the direction of stem cell fate, as in SMCs.[152,156] The micropatterned surface helps to mimic in vivo microenvironmental conditions of circumferential or helical SMC alignment within blood vessel walls.

Tay et al. investigated the differentiation of hMSCs toward the myogenic lineage when hMSCs were cultured on PLGA thin films with microstamped fibronectin in 20 μm stripes separated by nonadhesive gaps of 40 μm coated with Pluronic

F127.[133] Human MSCs cultured on micropatterned surfaces in expansion medium were found to be highly elongated with small adhesive areas of approximately 2000 μm^2, whereas hMSCs cultured on unpatterned surfaces had flat morphologies with large adhesive areas of approximately 10 000 μm^2.[133] Several hallmark neurogenesis (NeuroD1, nestin, GFAP, and MAP2) and myogenesis genes (GATA4, MyoD1, cTnT, and β-MHC) were upregulated in hMSCs on micropatterned surfaces in expansion medium, whereas osteogenic genes (alkaline phosphatase, RUNX2) were specifically downregulated or remained at normal levels. Myogenic lineage proteins, such as cardiac myosin heavy chain (MHC), predominantly existed in hMSCs cultured on micropatterned surfaces.[133] The enforced cell shape distortion resulted in the rearrangement of the cytoskeletal network and altered the shape of the nucleus, indicating the mechanical deformation of hMSCs translated into a biochemical response and ultimately contributed to specific differentiation toward a specific lineage, such as the myocardial lineage.

The differentiation of hESCs and hMSCs into endoderm lineages, such as hepatocytes and β cells, should be useful for clinical application but requires relatively difficult and complex procedures. Stimulation of stem cells with several growth factors and drugs is necessary at optimal concentrations with specific timing and duration. Tuleuova et al. developed a rather simple method of differentiating ESCs into the hepatic lineage by cultivating mESCs on micropatterned protein arrays with and without micropatterned coculture of human hepatic stellate cells.[155]

Protein microarrays were contact-printed on silane-modified glass slides using a microarray system with 500 μm-diameter circle-shaped protein spots in which the protein solution used for contact-printing was composed of hepatocyte growth factor (HGF), basic fibroblast growth factor (bFGF), and bone morphogenetic protein (BMP4) mixed with ECM composed of fibronectin and collagen type I.[155] Murine ESCs were cultured on the protein spots and exhibited hepatic differentiation. Coculture with nonparenchymal liver cells (hepatic stellate cells) on the protein spots enhanced hepatic differentiation of mESCs compared with mESC culture on the protein spots alone or with coculture of the hepatic stellate cells without micropatterning.[155] Microarrayed protein spots on dishes seem to guide or sort mESCs into hepatic lineages with high efficiency; hepatic differentiation of mESCs cultured on the printed protein spots was found to be enhanced compared with mESCs in conventional culture with media containing the same growth factors in soluble form.[155] Furthermore, a large amount of soluble growth factors were used in the conventional culture method, with daily media exchanges using media containing growth factors, while growth factors in the protein spots were printed once at the beginning of an experiment, with 60 times less total growth factor used than in the conventional culture medium.[155] This indicates that protein microarrays provide a more effective method of presenting functional growth factors to ESCs and allow more economical growth factor use. Growth factors bound to ECM and immobilized on the surface may have more stable and functional potential than soluble growth factors added to culture media.[155,162]

3.4. Neural Stem Cell Differentiation on Micropatterned Surfaces

Axonal regeneration in the central nervous system (CNS) is restricted by the inhibitory influences of the glial and extracellular environments after CNS injury.[153,163] Transplantation of NSCs and neural progenitor cells (NPCs) is a promising strategy for repairing the injured CNS. One instructive environment for axonal regeneration and restoration of function is the culture of NSCs, NPCs, or differentiated MSCs into neural cells on scaffolds with guidance channels.[128,134,153,154,164−166]

Ruiz et al. prepared PLL-micropatterned surfaces on Petri dishes coated with a plasma polymerized PEO using the microcontact printing method.[134] Various patterns of 1-nm-thick cell adhesive PLL were created on a cell-repellent PEO matrix. Neural stem cells cultured on the PLL patterns in differentiating medium over 20 days exhibited good confinement to the PLL domains.[134] Neural stem cells cultured on the PLL-micropatterned surface generated random axon-like projections outside of the patterns and expressed high amounts of neural markers in the differentiation medium. Migration and axon-like outgrowth were successfully guided by means of interconnected square patterns of PLL.[134]

Recknor et al. investigated directional growth and differentiation of adult rat hippocampal progenitor cells (AHPCs) on micropatterned PDMS substrates coated with PLL and laminin.[153] The micropatterned PDMS substrates had striped groove morphologies with 13 μm terrace widths, 16 μm groove widths, and 4 μm depths (Figure 11f). The micropatterned surface-directed AHPCs into over 75% alignment in the groove direction.[153] AHPCs were also cocultured with astrocytes, generating nearly double the percentage of cells (i.e., 35%) expressing class III β-tubulin (TuJ-1) on the micropatterned surface in comparison to those on nonpatterned surfaces or those growing in the absence of astrocytes.[153] This indicates that a physical biomaterial cue (micropatterned surface) in synergy with chemical (laminin) and biological (astrocytes) guidance cues facilitates the neuronal differentiation of AHPCs.[153] Integrating these cues seems to be important in understanding and controlling neural stem cell differentiation and in designing scaffolds for guided nerve generation in the future.

Microchannel surfaces patterned using photolithographic techniques have been reported to generate highly oriented neurites as described in the previous section.[167−169] However, most of these studies did not investigate the effects of the microstructure on stem cell differentiation into neural lineages. Beduer et al. investigated the effect of groove and terrace width of micropatterned surfaces with striped groove morphologies on the differentiation of human neural stem cells into neurons and intercommunication between neurons. In this study, hMSCs were cultured on the surfaces of micropatterned PDMS plates with varying dimensions of terrace (t) and groove (g) width: (a) t = 5 μm and g = 5 μm, (b) t = 10 μm and g = 10 μm, (c) t = 20 μm and g = 20 μm, and (d) t = 10 μm and g = 60 μm (Figure 11f).[135] The micropatterned PDMS plates were coated with PLL and laminin. A large majority of the adherent cells were located in the grooves and extended neurites inside the microgrooves along the walls.[170,171] Neuronal differentiation as evaluated by Tuj-1 immunostaining increased with increasing groove width, while adherent cell density did not depend on either groove or terrace width.[135] The differentiation of stem cells into neurons was especially affected and decreased on surfaces with micropatterned widths smaller than the cell soma diameter (12 μm). Furthermore, the size constraints imposed by the line microchannels of 5 μm−5 μm, 10 μm−10 μm, and 20 μm−20 μm caused a significant

decrease in the mean number of neurites per neuron compared with the control flat PDMS plates.[135] The micropatterning of neural stem cells seems to influence the number of neurites per neuron. Neuronal cells predominantly exhibited a single neurite (83%) when the cells were cultured on micropatterned surfaces with narrow terraces and grooves (t = 5 μm and g = 5 μm), while only 27% of neural cells had single neurites on micropatterned surfaces with wider terraces and grooves (t = 10 μm and g = 60 μm).[135] The proportion of neurons developing two or three neurites increased with the microchannel width. Neurite length was also affected by the microchannel width. A significant decrease in neurite length was observed on micropatterned surfaces with narrow grooves (t = 5 μm and g = 5 μm) compared with those with wider grooves (e.g., t = 20 μm and g = 20 μm or t = 10 μm and g = 60 μm).[135] Small micropatterns appeared to hinder neurite development.

As for neurite direction and orientation, neural cells preferentially aligned their neurites along the axes of the line patterns. Therefore, alignment was stronger in the smaller microchannels. The proportion of neurites forming angles smaller than 10° to the microchannel direction was 95% on surfaces with narrow grooves (t = 5 μm and g = 5 μm), whereas that same proportion decreased to 44% on surfaces with wide grooves (t = 10 μm and g = 60 μm).[135] Micropatterned surfaces with narrow channels (t = 5 μm and g = 5 μm) generated sharp neurite alignments parallel to the microchannel direction, while the differentiation rate and neurite length were drastically decreased.

Nanotopography may influence stem cell differentiation into specific lineages, such as neural lineages (neurons, astrocytes, and oligodendrocytes), because ECM in vivo has nanoscale topography in stem cell niches. Yim et al. cultured hMSCs on micropatterned and nanopatterned PDMS substrates with striped groove morphologies with (a) 700 nm terrace widths, 350 nm groove widths, and 350 nm depths, (b) 20 μm terrace widths, 1 μm groove widths, and 350 nm depths, (c) 20 μm terrace widths, 2 μm groove widths, and 350 nm depths, or (d) 20 μm terrace widths, 10 μm groove widths, and 350 nm depths.[126] The micropatterned and nanopatterned PDMS substrates were coated with collagen type I.

When hMSCs were cultured on nanopatterns with 350 nm groove widths in expansion medium where the groove size was 1 order of magnitude smaller than the cell body, hMSC nuclei and cell bodies were significantly elongated.[126] F-actin fibers were stretched predominantly along the long axis of the cells. The alignment of cells on nanopatterned surfaces was 86.5%, while no alignment was observed on unpatterned surfaces.[126] Gene expression and microarray studies showed that neuronal (SOX2, neurofilament light peptide [NFL], and tyrosine hydroxylase [TH]) and muscular (myosin light chain and myf5) gene markers were significantly upregulated on nanopatterned surfaces even in expansion medium; the changes in expression were not significant on unpatterned or micropatterned surfaces.[126] Notably, the mature neuronal markers microtubule associated protein 2 (MAP2) and TuJ-1 were also detected on nanopatterned surfaces in expansion medium. A significant terrace width dependency of neuron differentiation was observed on patterned surfaces.[126] MAP2 expression increased with decreasing groove width when hMSCs were cultured in expansion medium. Synaptophysin expression was detected in hMSCs cultured on nanopatterned surfaces in expansion and differentiation media (i.e., with retinoic acid) but not on unpatterned surfaces, suggesting synapse formation in the cells cultured on nanopatterned surfaces.[126]

These studies show that nanotopography plays an important role in regulating stem cell differentiation. Nanotopography alone can induce significant upregulation of neuronal markers in hMSCs, suggesting induction into the neuronal lineage.

3.5. Stem Cell Differentiation on Nanofiber Surfaces

Stem cell culture on nanofibers can be considered a sophisticated 3-D example of stem cell culture on nanopatterned surfaces. Furthermore, structural protein fibers, such as native collagen and elastin in tissue, have diameters ranging from several dozen to several hundred nanometers.[172,173] Nanoscaled protein fibers are entangled with each other and generate nonwoven protein fibers, providing tensile strength and elasticity in native tissue.[172] Therefore, stem cell culture on nanofibers can be considered to mimic the environment of the stem cell niche in vivo.

There are four types of nanofibers: (1) nanofibers formed by the self-assembly of peptide amphiphile molecules,[128,172,174−181] (2) nanofibers prepared by electrospinning, (3) nanofibers prepared by micro(nano)phase separation, and (4) nanofibers formed by self-assembly of ECMs such as collagen. Nanofibers prepared by the self-assembly of peptide amphiphile molecules have small diameters in the lower end of the range of natural extracellular matrix collagens, whereas nanofibers prepared with the electrospinning method have large diameters on the upper end of that range.[176] Nanofibers prepared using the microphase separation method have similar diameters to natural extracellular matrix collagens and have macropore structures.[176]

3.5.1. Stem Cell Differentiation on Nanofibers Formed by Self-Assembly of Amphiphile Peptides. Self-assembling peptides form nanofibers that can be controlled at physiological pH by altering salt concentration.[175] A transparent gel-like solid is formed by mixing cell culture medium (e.g., DMEM supplemented with 15% fetal bovine serum [FBS]) with peptide amphiphile solution (e.g., 1 wt %). The transparent gel-like solid solution is composed of nanofibers, as verified by atomic force microscopy in solution[178] and scanning electron microscopy in dried samples.[128,172,175,176,182] When these nanofiber hydrogels formed by self-assembling peptides undergo shear thinning, they quickly recover nearly 100% of their elastic modulus when the shearing force is released. Therefore, there is great potential that nanofiber hydrogels can be used as an injectable delivery agent of stem cells to injured sites in vivo.[128,181]

Several types of self-assembling peptides have been designed, and some examples are shown in Table 8.[128,172,175−178,180,183] Self-assembling peptides have hydrophobic and hydrophilic regions to create amphiphilic characteristics for the generation of self-assembled nanofibers. In most self-assembling peptides, the hydrophobic regions are composed of alkyl chain (e.g., $[CH_2]_{15}CH_3$) and RADA16 (i.e., $[RADA]_4$) or hydrophobic oligopeptides (e.g., $(Ala)_4(Gly)_3$ $[A_4G_3]$),[128] whereas the hydrophilic parts are composed of cell receptor-binding sequences, such as RGDS, DGEA, KRSR, IKVAV, YIGSR, etc. Some self-assembling peptides are designed to have biodegradable characteristics. For this purpose, an enzyme-degradable site for matrix metalloproteinase-2 (MMP-2), GTAGLIGQ (Gly-Thr-Ala-Gly-Leu-Ile-Gly-Gln), may also be included.[180] Table 9 summarizes various research studies on the differentiation of stem cells cultured on nanofibers formed by

Table 8. Sequences of Self-Assembled Peptide Amphiphile for Stem Cell Immobilization

name (model ECM)	chemical sequence	ref (year)
PA-RGDS (collagen I, fibronectin, osteopontin)	$CH_3(CH_2)_{14}$CONH-GTAGLIGQ-**RGDS**	180 (2009)
PA-DGEA (collagen I)	$CH_3(CH_2)_{14}$CONH-GTAGLIGQ-**DGEA**	180 (2009)
PA-KRSR	$CH_3(CH_2)_{14}$CONH-GTAGLIGQ-**KRSR**	180 (2009)
PA-RGES (dummy of RGDS)	$CH_3(CH_2)_{14}$CONH-GTAGLIGQ-RGES	180 (2009)
PA-S (control)	$CH_3(CH_2)_{14}$CONH-GTAGLIGQ-S	180 (2009)
IKVAV-PA (laminin)	**IKVAV**-Glu(E)-$A_4G_3(CH_2)_{15}CH_3$	128 (2004)
EQS-PA (control)	EQS-Glu(E)-$A_4G_3(CH_2)_{15}CH_3$	128 (2004)
RGD-PA (collagen I, fibronectin, osteopontin)	**RGD**-Glu(E)-$A_4G_3(CH_2)_{15}CH_3$	172 (2006)
RGD-PA (collagen I, fibronectin, osteopontin)	**RGD**-Glu(E)-$A_4G_3(CH_2)_{15}CH_3$	176 (2006)
RADA16-PDSGR (laminin)	Ac-$(RADA)_4$-GG**PDSGR**-$CONH_2$	175 (2006)
RADA16-SDPGYIGSR (laminin)	Ac-$(RADA)_4$-GG**SDPGYIGSR**-$CONH_2$	175 (2006)
RADA16-IKVAV (laminin)	Ac-$(RADA)_4$-GG**IKVAV**-$CONH_2$	175 (2006)
RADA16-SKPPGTSS (bone marrow homing)	Ac-$(RADA)_4$-GG**SKPPGTSS**-$CONH_2$	175 (2006)
RADA16-PFSSTKT (bone marrow homing)	Ac-$(RADA)_4$-GG**PFSSTKT**-$CONH_2$	175 (2006)
RADA16-FLGFPT (bone marrow homing)	Ac-$(RADA)_4$-GG**FLGFPT**-$CONH_2$	175 (2006)
RADA16-DGEA (collagen I)	Ac-$(RADA)_4$-GG**DGEA**-$CONH_2$	175 (2006)
RADA16-RGDS (collagen I, fibronectin, osteopontin)	Ac-$(RADA)_4$-GG**RGDS**-$CONH_2$	175 (2006)
RADA16-FPGERGVEGPGP (collagen I)	Ac-$(RADA)_4$-GG**FPGERGVEGPGP**-$CONH_2$	175 (2006)
RADA16-PRGDSGYRGDSG (collagen VI)	Ac-$(RADA)_4$-GG**PRGDSGYRGDSG**-$CONH_2$	175 (2006)
RADA16 (control)	Ac-$(RADA)_4$-$CONH_2$	175 (2006)
MMP2-RGDS (collagen I, fibronectin, osteopontin)	Ac-GTAGLIGQ**ERGDS**	177 (2008)
MDP-RGDS (collagen I, fibronectin, osteopontin)	Ac-EESLSLSLSLSLSLEE**GRGDS**-CO-NH_2	183 (2011)
RADA16-RGDSP (collagen I, fibronectin, osteopontin)	Ac-$(RADA)_4$-**RGDSP**	178 (2010)

the self-assembly of peptide amphiphile molecules.[128,172,174,176,178,180,184]

Anderson et al. prepared peptide amphiphile nanofibers inscribed with specific cellular adhesive ligands (i.e., RGDS, DGEA, and KRSR) and investigated whether they could direct osteogenic differentiation of hMSCs without osteogenic supplements.[3,180] The peptide amphiphile nanofibers were used to create self-assembled 2-D coatings on cell culture dishes. Human MSCs cultured on RGDS-containing peptide amphiphile nanofibers, but not DGEA- or KRSR-containing nanofibers, exhibited significantly greater alkaline phosphatase activity, indicating early promotion of osteogenic differentiation, and showed a progressive shift toward osteogenic morphology and positive staining for mineral deposition.[3,180] The peptide amphiphile nanofibers, which mimic the native ECM in bone, were found to direct the osteogenic differentiation of hMSCs to a certain degree without the aid of supplements and provided an adaptable environment that allowed various adhesive ligands to control cellular behaviors.[3,180]

Silva et al. prepared a 3-D network of nanofibers formed by the self-assembly of peptide amphiphile molecules (IKVAV-PA in Table 8) in which neural progenitor cells were encapsulated in vitro.[128] The neurite-promoting laminin epitope IKVAV (isoleucine-lysine-valine-alanine-valine) was included in the peptide amphiphile molecules. Self-assembly was triggered by mixing cell suspensions in media and peptide amphiphile molecules. The resulting self-assembled nanofibers placed the bioactive epitopes (IKVAV) on their surfaces at van der Waals packing distances and produced a gel-like solid containing 99.5 wt % water.[128] The nanofibers had high aspect ratios and large surface areas; they were 5−8 nm in diameter and ranged from hundreds of nanometers to a few micrometers in length. Thus, these nanofibers were able to present the IKVAV epitopes to neural progenitor cells at an extremely high density relative to natural laminin ECM.[128]

Neurite length and cell-body area within the nanofiber networks were found to be noticeably larger than in neurons cultured on 2-D dishes.[128] Neural progenitor cells were found to differentiate into neurons on the self-assembled nanofiber scaffolds, in contrast to cells cultured on laminin-coated or poly(D-lysine)-coated dishes, which suppressed astrocyte differentiation.[128] It was found that the physical entrapment of IKVAV in the self-assembled nanofibers, not solely its presence in the scaffold, was important to the neuronal differentiation of neural progenitor cells because the addition of IKVAV-soluble peptide into gels containing neural progenitor cells where the IKVAV sequence had been changed into the nonbioactive sequence of EQS (glutamic acid−glutamine−serine) did not promote selective neuron differentiation.[128]

Gelain et al. also prepared 3-D networks of nanofibers, formed by the self-assembly of peptide amphiphile molecules with several functional motifs, including cell adhesion (SDPGYIGSR and IKVAV as laminin models, RGDS as a fibronectin model, and FPGERGVEGPGP as a collagen type I model), differentiation, and bone marrow homing (SKPPGTSS, PFSSTKT, and FLGFPT) motifs, in which neural progenitor cells were encapsulated in vitro.[175] The peptide amphiphile nanofiber gels with bone marrow homing motifs (SKPPGTSS and PFSSTKT) enhanced neural cell survival without added soluble growth factors or neurotrophic factors in the culture medium.[175] The populations of β-III tubulin$^+$ (neuron) (superscript of "+" indicates the expression of this protein or gene), GFAP$^+$ (astrocyte), and Nestin$^+$ (neural progenitor) cells cultured on peptide amphiphile nanofiber gels with the appropriate motifs were significantly larger than those in conventional 2-D culture (i.e., TCPS) and were similar to those cultured on Matrigel.[175] Matrigel is composed of isolated components from the sarcomas of Engelbreth−Holm−Swarm mice,[2,185,186] including laminin, collagen type IV, heparan sulfate proteoglycans, enactin, and growth factors (e.g., TGF-β, EGF, and FGF). Matrigel contains unknown ingredients and is extracted from mice, whereas synthetic peptide amphiphiles are chemically defined. These are important considerations for the clinical application of stem cell scaffolds, although Matrigel is an attractive biomaterial for the maintenance of stem cell pluripotency[2] or the specific differentiation of stem cells.[187,188] Self-assembling peptide nanofiber gels prepared by Gelain et al. can mimic the characteristics of Matrigel to guide stem cell differentiation into specific lineages.[175] They succeeded in guiding neural stem cells

Table 9. Some Research Studies for Stem Cell Differentiation on Nanofiber Materials Prepared by Self-Assembled Peptide Amphiphile[a]

stem cell source	self-assembled peptide amphiphile for nanofiber preparation	medium	differentiation	ref (year)
hMSCs	oligopeptides containing RGDS, DGEA, or GRES	differentiation medium	osteoblasts	180 (2009)
rat MSCs	oligopeptides containing RGD	differentiation medium	osteoblasts	172 (2006)
rat MSCs	oligopeptide containing RGDS	differentiation medium	osteoblasts	176 (2006)
human dental pulp stem cells, stem cells from human exfoliated deciduous supplements	oligopeptide containing RGDS (GTAGLIGQERGDS)	differentiation medium	osteoblasts	177 (2008)
rat marrow-derived cardiac stem cells	oligopeptides containing RGDSP	expansion medium	cardiomyocytes	178 (2010)
rat cardiac progenitor cells	oligopeptides containing insulin-like growth factor-1	expansion medium	cardiomyocytes	174 (2009)
murine neural progenitor cells	oligopeptides containing IKVAV	expansion medium	neuronal cells	128 (2004)
murine NSCs	oligopeptides containing IKVAV, YIGSR, DGEA, RGDS, PDSGR	differentiation medium	neural cells	175 (2006)

[a]MSCs, mesenchymal stem cells; hMSCs, human MSCs; NSCs, neural stem cells.

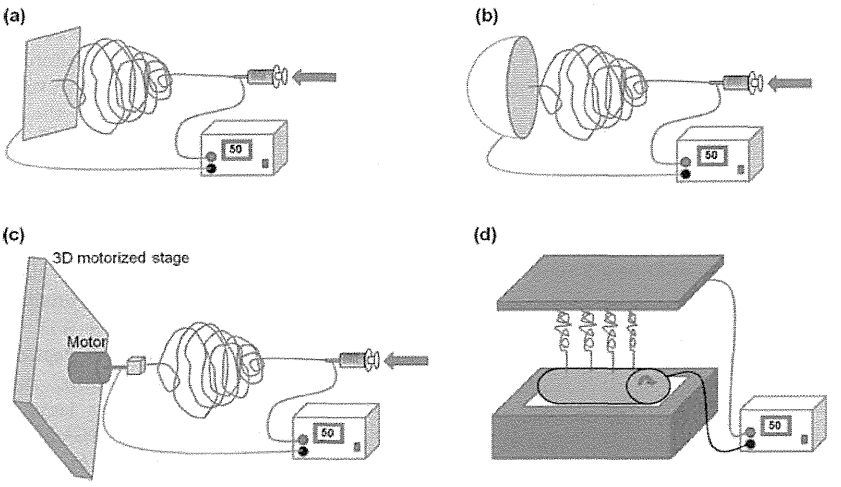

Figure 15. Typical examples of electrospinning methods. Traditional electrospinning method to prepare nonwoven fabric scaffolds (a), the electrospinning method to prepare cotton ball-like scaffolds (b), the electrospinning method to prepare double-layered 2-D architectures (crosshatch pattern) using a 3-D stage (c), and the Nanospider electrospinning method (d).

into neural and glial differentiation without the addition of extra growth factors by entrapping the neural stem cells in self-assembled peptide amphiphile nanofiber gels.

Hosseinkhani et al. prepared a 3-D network of nanofibers formed by the self-assembly of peptide amphiphile molecules containing RGD sequences (RGD-PA in Table 8) in which rat MSCs were encapsulated in vitro.[176] A 3-D nanofiber network was also formed in a hydrogel by mixing MSC suspensions in media with dilute aqueous solutions of the peptide amphiphile. The attachment, proliferation, and osteogenic differentiation of MSCs were successfully facilitated in the peptide amphiphile nanofiber gels with and without RGD sequences in comparison to MSCs in conventional 2-D culture on cell culture dishes.[176] However, the presence of the RGD sequence in the self-assembled amphiphile nanofibers enabled MSCs to promote greater attachment, proliferation, and osteogenic differentiation in comparison to those without the RGD sequence. This result can be explained by the possibility that binding of MSC integrin receptors with the RGD of the peptide amphiphile enhanced cell attachment, along with proliferation and osteogenic differentiation, on the nanofibers.[176]

The 3-D scaffolds used in conventional tissue engineering require surgery for their implantation, which is undesirable for clinical applications. Gel scaffolds consist of nanofiber networks formed by the aggregation of the peptide amphiphiles, and the process is physically triggered by the addition of a cell suspension to the aqueous peptide amphiphile solution. The gels formed by this process could be delivered to injured tissue by injecting the combined cell suspension and peptide amphiphile solution, allowing the injected solution to form a gel at the injection site.[176,177]

Self-assembling peptide nanofiber gels will be useful for the 3-D culture of stem cells in tissue engineering and in general molecular and cell biology.

3.5.2. Stem Cell Differentiation on Nanofibers Prepared by Electrospinning. Electrospun nanofibers can be generated from a spinning nozzle when high voltage is applied between the spinning nozzle and a flat metal collector. Several different nanofiber morphologies can be prepared with

Table 10. Some Research Studies for Stem Cell Differentiation on Nanofibers Prepared by Electrospinning[a]

stem cell source	materials for stem cell culture	medium	differentiation	ref (year)
hMSCs	PCL nanofibers	differentiation medium	osteoblasts, chondrocytes, adipocytes	201 (2005)
hMSCs	PLLA nanofibers	differentiation medium	osteoblasts	203 (2005)
hMSCs	nonwoven collagen type I nanofibers (diameter (d) = 50−200, 200−500, and 500−1000 nm)	differentiation medium	osteoblasts	191 (2006)
hMSCs	nanofibers composed of nanosized demineralized bone powders with PLLA composite material	differentiation medium	osteoblasts	192 (2008)
hMSCs	BMP-2-incorporated PLLA nanofibers	differentiation medium	osteoblasts	204 (2008)
hADSCs	collagen type I nanofibers	differentiation medium	osteoblasts	193 (2008)
hMSCs	PLLA-collagen I blend nanofibers	differentiation medium	osteoblasts	194 (2009)
hUSSC	plasma-treated PLLA nanofibers coated with nanohydroxtapatite	differentiation medium	osteoblasts	195 (2010)
hMSCs, hAFSCs	PCL nanofibers	differentiation medium	osteoblasts	202 (2010)
rabbit MSCs	nanofibers composed of nanosized hydroxyapatite and PCL having 340 nm diameter	differentiation medium	osteoblasts	196 (2011)
hUSSC	plasma-treated or collagen-grafted PES nanofibers	differentiation medium	osteoblasts	197 (2011)
hMSCs	nonwoven PLGA nanofibers with an diameter of 760 nm	differentiation medium	osteoblasts, chondrocytes	198 (2007)
MSCs	PLLA nanofibers	differentiation medium	chondrocytes	205 (2008)
calf MSCs	PCL nanofibers	differentiation medium	fibrocartilagious cells	199 (2011)
hMSCs	aligned and randomly oriented nanofibers prepared from thermally responsive hydroxybutyl chitosan	expansion medium	myocytes	69 (2007)
hATSPCs	aligned and randomly oriented PLLA nanofibers	expansion and differentiation medium	tendon	200 (2010)
murine ESC (CE3, RW4)	alighned and randomly oriented PCL nanofibers	differentiation medium	neural cells	68 (2009)
hMSCs	PLCL/collagen nanofibers	differentiation medium	neural cells	206 (2009)
rat ANSCs	PLO and laminin coated PCL nanofibers by electrospinning (d = 260, 480, 930 nm)	differentiation medium	neural cells	182 (2010)
mouse NSCs (C17.2)	collagen nanofiber cross-linked with rose bengal as photoinitiator by laser irradiation	expansion medium	neuronal cells	207 (2010)
rat NSCs	aligned, single- and double layer polystyrene nanofiber meshes coated with PLO and laminin (d = 800 nm)	expansion medium	neuronal lineages	76 (2011)
hESCs	PLO/laminin-coated PCL	expansion medium	neural cells	208 (2011)
hMSCs	PCL-gelatin nanofibers immobilized retinoic acid (d = 240−280 nm)	expansion medium	neural cells	71 (2012)
hESCs	tusan silk fibroin nanofibers coated with poly-D-lysine (PDL)/laminin (d = 400 and 800 nm)	differentiation medium	neuronal cells	209 (2012)
UCBPCs	aminated PES nanofibers	differentiation medium	endothelial and smooth muscle cells	210 (2009)
rat MSCs	photopolymerized PEG nanofibers coated with collagen type I	expansion medium	endothelial and smooth muscle cells	70 (2012)
rat MSCs	PLGA and collagen nanofibers immobilized CD29 antibody	expansion medium	epidermal cells	211 (2011)
hUSSCs	oxygen-plasma treated nanofibers of poly(ε-caprolactone)	differentiation medium	hepatocytes	212 (2009)
hMSCs	collagen-grafted PLLA nanofibers	differentiation medium	hepatocytes	213 (2012)
murine limbal stem cells, MSCs	polyamide 6/12 nanofibers by electrospinning (d = 290−539 nm)	expansion medium	proliferation and transplantation into damaged ocular surface	214 (2012)

[a]MSCs, mesenchymal stem cells; hMSCs, human MSCs; hADSCs, human adipose-derived stem cells; hUSSC, human unrestricted somatic stem cells; hAFSCs, human amniotic fluid stem cells; hATSPCs, human fetal achilles tendon stem/progenitor cells; NSCs, neural stem cells; ESCs, embryonic stem cells; hESCs, human ESCs; ANSCs, adult neural stem cells; UCBPCs, UCB-derived progenitor cells ($CD133^+$ cells); PES, polyethersulfone; PLC, poly(ε-caprolactone); PLCL, poly(L-lactic acid-*co*-3-caprolactone); PLGA, poly(lactic acid-*co*-glyconic acid); PLLA, poly(L-lactic acid), PLO, poly(L-ornithine).

dx.doi.org/10.1021/cr300426x | Chem. Rev. 2013, 113, 3297−3328

the electrospinning method, such as nonwoven fabric-like sheets, oriented fabric-like sheets, and structures resembling cotton balls. The typical electrospinning method is schematically shown in Figure 15a. Electrospun products are flat and highly interconnected scaffolds with a nonwoven fabric sheet-like morphology in most cases.[3] These characteristics hinder cell infiltration and growth throughout the scaffold. Blakeney et al. developed a three-dimensional cotton ball-like electrospun scaffold consisting of low-density, uncompressed nanofibers.[189] A grounded spherical dish and an array of needle-like probes were used instead of a traditional flat-plate collector to create a cotton ball-like scaffold (Figure 15b).[3] Scanning electron microscopy revealed that the cotton ball-like scaffold consisted of electrospun nanofibers with similar diameters but larger pores and less-dense structures than traditional electrospun scaffolds.[189] These cotton ball-like structures will be interesting for use as scaffolds for guiding specific stem cell differentiation lineages. Aligned nanofibers prepared using the electrospinning method have also been reported (Figure 15c). The rotating fiber collector enables nanofibers to align with one another. Double-layer 2-D architecture (crosshatch pattern) can be achieved by orthogonal substrate orientation and repeated nanofiber deposition.

One of the disadvantages of nanofiber fabrication with the electrospinning method is the extremely low production speed. To solve this problem, a rotating metallic drum dipping into polymer solution was used as a spinning nozzle to fabricate multiple nanofibers from the drum instead of a single-nozzle spinning needle (Nanospider, Figure 15d).[190] In the future, this new technique may contribute to the production of nanofiber scaffolds on an industrial scale.

Table 10 summarizes nanofibers fabricated with the electrospinning method for stem cell differentiation that have been reported in the literature.[68−71,76,182,191−214]

In general, human MSCs are difficult to differentiate into chondrocytes in 2-D monolayer culture. Pellet and hanging drop culture of hMSCs are the gold standards for chondrogenic differentiation.[215] This is likely because high seeding density leads to greater chondrogenic differentiation. Cell−cell contact and autocrine growth factors are important in chondrogenesis. Condensation of hMSCs initiates chondrogenesis during skeletal development,[216] suggesting the rationale for chondrogenic high-density pellet cultures.[217,218] Furthermore, the cell morphology in pellet and hanging drop culture is round as opposed to spread, as it is in monolayer culture. Morphological regulation is also an important parameter promoting hMSC chondrogenesis.[3]

Nanofibers fabricated with the electrospinning method have high surface area-to-volume ratios that maximize cell−material contact. Several researchers have reported that hMSCs on electrospun nanofibers can differentiate into chondrocytes, osteoblasts, and adipocytes.[191,195,198,201,205] Xin reported that hMSCs could differentiate into both chondrocytes and osteoblasts, depending on the induction media, when they were cultured on PLGA nanofibers. These results are important for tissue engineering applications for osteoarthritis because of the continuous differentiation of hMSCs into osteoblasts and chondrocytes.[198]

3.5.2.1. Effect of Nanofiber Size on Stem Cell Differentiation. Shih et al. prepared collagen type I nanofibers of varying diameters (50−200, 200−500, and 500−1000 nm) using the electrospinning method upon which hMSCs were seeded and examined for morphology, growth, adhesion, cell motility, and osteogenic differentiation.[191] Cells on all nanofiber sizes had more polygonal and flattened cell morphologies than those on TCPS. Moreover, hMSCs grown on 500−1000 nm nanofibers had significantly higher cell viabilities than TCPS controls.[191]

Christopherson et al. investigated the impact of nanofiber diameter on the differentiation of adult rat hippocampal-derived NSCs.[76,219] They found that NSCs cultured on smaller diameter (i.e., 283 nm) fibers differentiated preferentially into oligodendrocyte precursors in the presence of retinoic acid in medium containing serum, while NSCs preferentially differentiated into neuronal precursors on larger diameter fibers (i.e., 749 nm).

3.5.2.2. Effect of Nanofiber Alignment on Stem Cell Differentiation. Bakhru et al. prepared highly aligned, single-layer (uniaxially aligned) and double-layer (crosshatch pattern) polystyrene nanofiber meshes and investigated NSC fate as influenced by the physical microenvironment of the cells. Aligned nanofibers coated with poly(L-ornithine) (PLO) and laminin induced polarized NSC morphology and cellular elongation in the direction of fiber alignment, important for NSC neuronal differentiation.[76] The aligned fiber substrates promoted NSC neuronal lineage differentiation with an efficiency of 82.3%, whereas NSCs on conventional flat TCPS preferentially differentiated into glia (astrocytes) and not into neuronal lineages (efficiency of only 7%).[76] This research shows that microenvironmental physical cues determine stem cell differentiation fate.

Mahairaki reported that hESC-derived neural precursors (NPs) cultured on aligned fibrous substrates exhibited a higher rate of neuronal differentiation than those on other matrices; 62% and 86% of NPs become TUJ-1$^+$ cells (early neurons) on aligned microfibers and nanofibers, respectively, whereas only 32% and 27% of NPs acquired the same fate on random microfibers and nanofibers, respectively.[208]

Xie et al. induced mouse ESCs to differentiate into neural progenitor cells (NPCs) by adding retinoic acid to embryoid bodies (EBs). They examined biodegradable PCL nanofiber scaffolds seeded with neural progenitor cells and found culturing EBs on uniaxially aligned PCL nanofibers enhanced differentiation into neural lineages and promoted neurite outgrowth in comparison to EBs cultured on randomly oriented PCL nanofibers.[68] Neurites differentiated from EBs on aligned nanofibers extended along the direction of nanofiber alignment, while neurites cultured on randomly oriented nanofibers extended in all directions. More astrocytes were present on randomly oriented nanofibers than on aligned nanofibers.[68] The maximum length of neurite projections from EBs cultured on aligned nanofibers was significantly higher (500 μm longer) than that of neurites on randomly oriented nanofibers.[68] Aligned nanofibers seem to be able to enhance both the rate of EB neurite extension and neurite outgrowth direction.

Lim et al. also reported that higher fractions of adult rat NSCs on aligned PCL nanofibers coated with PLO and laminin exhibited neuronal differentiation compared with cells on randomly aligned PCL nanofibers or unpatterned surfaces.[182] Aligned nanofiber meshes 480 nm in diameter yielded the highest fraction of neural progenitors among nanofibers with 260, 480, and 930 nm diameters. This effect was in part due to neuron substrate selectivity, whereby aligned fiber substrates were less receptive to the attachment and survival of

oligodendrocytes than were randomly oriented fibers or unpatterned substrates.[182]

Aligned PCL–gelatin nanofibers (average diameter (d) = 270 nm) encapsulated with up to 0.3 wt % retinoic acid (RA) were prepared by Xu et al as scaffolds for hMSCs differentiated into neuronal lineages.[71] These nanofibers released RA for at least 14 days. Human MSCs cultured on aligned PCL–gelatin nanofibers with and without RA encapsulation upregulated expression of neural markers Tuj-1 (neuronal marker), MAP2 (mature neuronal marker), GalC (oligodendrocyte marker), and RIP (mature oligodendrocyte) (Table 2) at the mRNA and protein levels in comparison to hMSCs cultured on conventional TCPS or on randomly orientated PCL–gelatin nanofibers.[71] Human MSCs cultured on aligned PCL–gelatin nanofibers with encapsulated RA showed significantly enhanced neural marker expression in comparison to hMSCs on aligned PCL–gelatin nanofibers without RA encapsulation or randomly oriented PCL–gelatin nanofibers with encapsulated RA.[71] In particular, hMSCs cultured on aligned PCL–gelatin nanofibers with encapsulated RA, which allowed the controlled release of RA with lower loading amounts (>8 times lower), enhanced MAP2 and RIP expression compared with hMSCs cultured on nanofibers without RA encapsulation in culture medium containing high amounts of RA.[71] Higher expression of the mature neuronal marker MAP2 in hMSCs cultured on aligned PCL–gelatin nanofibers with encapsulated RA compared with the expression of glial markers at the mRNA and protein levels suggested that these nanofibers enhanced hMSC neuronal differentiation. Furthermore, positive staining for synaptophysin was detected only in cells cultured on aligned PCL–gelatin nanofibers with encapsulated RA.[71] These results illustrate the advantage of the nanofiber-based approach in enhancing the neuronal differentiation potential of hMSCs and demonstrate the importance of the drug delivery approach in directing stem cell fate. Such biomimicking drug-encapsulating nanofibers (used as scaffolds) may permit subsequent direct cell transplantation and may provide guidance cues to control the fate of endogenously recruited stem cells.

Dang and Leong prepared aligned nanofibrous scaffolds composed of a thermally responsive hydroxybutyl chitosan (HBC) blended with and without collagen type I.[69] Cell sheets could be generated by cooling hMSCs cultured on these scaffolds to 4 °C, allowing the cells in the polymer-free cell sheets to retain their elongated cell morphology and cytoskeletal alignment. The expression profiles of genes representative of three separate hMSC differentiation lineages were evaluated in the aligned hMSC cell sheets, where hMSCs were cultured on aligned HBC fiber scaffolds with and without collagen type I in proliferation medium and not in differentiation induction medium. These lineages included osteogenic, chondrogenic, and myogenic differentiation.

Expression of genes from all three differentiation lineages was detected in hMSCs cultured on both aligned HBC and HBC/collagen nanofibrous scaffolds. Interestingly, a definitive upregulation of myogenic genes was apparent for hMSCs on the aligned nanofibrous scaffolds when the genes expressed by hMSCs cultured on HBC films and TCPS were compared. Although MyoD expression was not detected in hMSCs on aligned nanofibrous scaffolds, elevated levels of myogenin, a gene involved in muscle differentiation and downstream of MyoD expression, suggested myogenic commitment.[69] The aligned nanofibrous topography induced an elongated nuclear shape, and this elongated nuclear shape was considered to be a major factor in the hMSC myogenic induction. The aligned nanofibers provide topographical cues to induce cell alignment, potentially guiding gene expression and influencing stem cell differentiation fate.

Tendons are specific connective tissues composed of parallel collagen fibers. It is known that human tendon stem/progenitor cells (hTSPCs) reside within a niche composed primarily of parallel collagen fibers and that this niche plays an important role in regulating their function and differentiation.[200,220–222] ECM or polymer electrospinning may be a suitable method to directly replicate the natural tendon ECM. Therefore, Yin et al. fabricated aligned and randomly oriented PLLA fibrous scaffolds, cultured hTSPCs on them, and evaluated the regulation of hTSPC orientation and differentiation into tendon by the aligned electrospun nanofibers.

Human TSPCs displayed spindle-shaped morphologies and were well-oriented on the aligned nanofibrous scaffolds. The expression of tendon-specific genes (Eya 2 and scleraxis) was significantly higher in hTSPCs cultured on aligned nanofibers compared with those on randomly oriented nanofibrous scaffolds in proliferation media and even in osteogenic media (due to tenogenesis and osteogenesis sharing a common signaling pathway).[223] In addition, alkaline phosphatase activity and alizarin red staining showed that hTSPCs on randomly oriented nanofibrous scaffolds experienced induced osteogenesis, while those on aligned nanofibrous scaffolds displayed hindered osteogenic differentiation.

In in vivo experiments, hTSPCs on aligned nanofibrous scaffolds were transplanted subcutaneously into immunocompromised mice. The efficacy of seeding hTSPCs on aligned nanofibrous scaffolds in inducing tendon tissue regeneration in vivo was investigated. From the observation of hematoxylin and eosin (H & E) and Masson's trichrome staining, it was determined that aligned nanofibers induced the formation of spindle-shaped cells and tendon-like tissue. These results suggest that aligned electrospun nanofibrous scaffolds provide an instructive microenvironment for hTSPC differentiation into tendon-like tissue and may lead to the development of desirable, intelligently engineered tendons.

3.5.2.3. Stem Cell Differentiation on Hybrid Nanofibers. Bone structure is composed of highly organized nanofibrillar proteins (mainly consisting of collagen type I), which serve as a pattern for the deposition of crystalline calcium phosphate minerals in the form of hydroxyapatite (HA).[195,224] A combination of nanofibrous organic and inorganic composite scaffolds, such as (a) calcium phosphates with nanofibrous scaffolds[195,196] and (b) composite nanofiber scaffolds with nanosized demineralized bone powders and biodegradable polymer,[192] may have promising potential for bone tissue engineering applications. Seyedjafari et al. prepared electrospun PLLA nanofibers coated with nanohydroxyapatite (n-HA) and investigated the capacity of these fabricated scaffolds for bone formation in vitro using human cord blood-derived unrestricted somatic stem cells (USSCs) under osteogenic induction.[195] Nanofibers coated with n-HA (n-HA/PLLA) supported attachment, spreading, and proliferation of USSCs. Higher ALP activity (an early marker of osteogenesis), biomineralization, and bone-related gene (Runx2, osteonectin, osteocalcin) expression were observed on nanofibers coated with n-HA compared with PLLA scaffolds without n-HA coating.[195] Furthermore, the expression levels of these markers were higher in USSCs on PLLA nanofibers than in those on TCPS. In addition, nanofiber scaffolds coated with n-HA demonstrated

the capacity for ectopic bone formation in the absence of exogenous cells in vivo after subcutaneous implantation of the nanofiber scaffolds into mice.[195]

Chen et al. also prepared nanocomposite scaffolds of n-HA dispersed in PCL using the electrospinning method.[196] Osteogenic differentiation of MSCs was enhanced on the composite nanofibers with an increase in n-HA content of up to 50%.[196] The extent of mineralization was significantly greater in nanocomposite scaffolds with 50% n-HA, which have Ca/P ratios similar to bone.

Nanofibrous organic and inorganic composite scaffolds containing demineralized bone powders (DBP) and PLLA were developed using the electrospinning method by Ko et al.[192] PLLA/DBP and PLLA scaffolds were transplanted into a full-thickness bony defect created in the central part of the rat cranial bone (8 mm diameter). Their results revealed that a larger amount of newly formed bone extended across the defect area 12 weeks after implantation with PLLA/DBP scaffold transplantation than in rats without implants and in PLLA scaffolds and that the defect size was almost 90% smaller.[197] Therefore, PLLA/DBP composite nanofiber scaffolds may serve as favorable matrices for the regeneration of bone tissue. The defect size decreased to 10% of its original size when PLLA/DBP composite nanofiber scaffolds were transplanted.[197]

Nanofibrous organic and inorganic composite scaffolds seem to be suitable for guiding MSCs into osteoblasts and for generating the mineralization of MSCs intended for bone tissue engineering.

Fibrocartilaginous tissues such as the meniscus serve critical load-bearing roles and rely on arrays of collagen fibers to resist tensile loads encountered during normal activity. The tissues of these structures are frequently injured and possess limited healing capacity; therefore, there exists demand for tissue-engineered replacements.[199] Baker et al. investigated scaffolds composed of aligned nanofibers that directed bovine MSC orientation and the formation of organized ECM under mechanical stimulation with the goal of recreating the structural features of these anisotropic tissues in vitro.[199] They examined the effect of cyclic tensile loading on MSC-laden nanofibrous PCL scaffolds made using the electrospinning method.[199] MSC fibrous gene expression (collagen type I, fibronectin, lysyl oxidase) and collagen deposition increased with mechanical stimulation, and the tensile modulus also increased by 16% relative to controls.[199] These results show that dynamic tensile loading enhances the maturation of MSC-laden aligned nanofibrous constructs, suggesting that recapitulation of the structural and mechanical environment of load-bearing tissues results in increases in functional properties that can be exploited for tissue engineering applications.[199]

3.5.3. Stem Cell Differentiation on Nanofibers Prepared Using Phase Separation. The phase separation method is a typical way to prepare porous membranes with pore sizes ranging from 1 nm to 10 μm. However, the porosity of membranes with pore sizes on the order of nanometers is extremely low under typical conditions (e.g., less than 10%), making them inadequate for use as cell culture scaffolds. Several researchers have created nanofiber scaffolds rather than porous membranes using phase separation techniques. These scaffolds have promise for the culture and differentiation of stem cells, although there have been only a few reports describing stem cell culture and differentiation on nanofibers prepared using phase separation techniques compared with those created by self-assembly of peptide amphiphiles or using the electrospinning method. This is because nanofiber scaffolds prepared using the phase separation method are quite similar to the 2-D structure of nanofiber mats, and stem cells cannot migrate inside the nanofiber scaffolds (mats) and must remain on the surface.

Nanofiber matrices are typically prepared from synthetic polymers as follows: (1) synthetic polymer is dissolved in a "good" solvent; (2) the polymer solution is cast on plates or dishes and phase-separated by cooling; (3) the polymer solution (gel) is immersed in water, and the solvent is removed from the gel, generating nanofiber scaffolds (mats); and (4) the nanofiber matrices are washed and then freeze-dried.

Smith et al. prepared nanofiber matrices using PLLA with the phase separation method to mimic the morphology of natural ECM. Their goal was to examine the contribution of ECM morphology to the differentiation of murine ESCs because natural ECM, such as collagen type I, typically has a nanofiber morphology.[225] The resulting nanofiber matrices had an average fiber diameter of 150 nm and a porosity of 92.9%. ESCs cultured on the nanofiber matrices displayed more extended morphologies than those on films prepared from the same PLLA and those on gelatin-coated control dishes. Furthermore, ESCs cultured on nanofiber matrices exhibited higher Brachyury expression, indicating mesoderm differentiation, and had stronger expression of osteogenic genes (also mesoderm), such as collagen type I, Runx2, osteocalcin, and bone sialoprotein; however, they expressed less nestin (a neural marker, ectoderm) and TUJ-1 (a neuronal marker, ectoderm) than ESCs cultured on PLLA films or gelatin-coated dishes (control experiments). It was found that osteogenic differentiation was more highly promoted when ESCs were cultured on the nanofiber matrices than on film or gelatin-coated dishes. The mechanism of the enhanced osteogenic differentiation observed on the nanofiber matrices was partially explained by high adsorption of serum proteins and fibronectin on the nanofibers prepared from PLLA. Several integrin subunits associated with cellular adhesion to collagen type I ($\alpha2\beta1$) and fibronectin ($\alpha5\beta1$) were upregulated on the nanofiber matrices compared with the film.[225] The increase in $\beta1$ integrin transcription in ESCs on nanofiber matrices compared with those on film and gelatin-coated dishes supports increased mesoderm differentiation because increased $\beta1$ integrin on stem cells is directly related to increased mesoderm differentiation while inhibiting neural differentiation.[226] Increased fibronectin adsorption on the nanofiber matrices compared with the film and gelatin-coated dishes likely accelerates ESC differentiation to the mesoderm and osteogenic lineages, as supported by $\alpha5$ blocking experiments.[225] The nanofiber matrices had larger surface areas than the film and conventional flat culture dishes, which is favorable for the high adsorption of serum or ECM proteins. High, somewhat specific adsorption of serum and ECM proteins on nanofiber matrices prepared from selected chemical structures will be useful in designing dishes suitable for stem cell differentiation into specific lineages.

Polyhydroxyalkanoates (PHA) such as poly(3-hydroxybutyrate) (PHB), 3-hydroxybutyrate and 4-hydroxybutyrate (P4HB) copolymer, 3-hydroxybutyrate and 4-hydroxyhexanoate (PHBHHx) copolymer, and 3-hydroxybutyrate and 4-hydroxybutyrate (PHB4HB) copolymer are reported to have good biodegradability and no cytotoxicity in vitro and in vivo.[227,228] Xu et al. prepared nanofiber matrices using PHA,

which is structurally similar to natural ECM.[227] Rat NSCs were cultured on PHA nanofiber matrices and films. The viability of NSCs on PHA nanofiber matrices was significantly higher than that of those on PHA films.[227] This result indicates that nanofiber matrices with a 3-D nanostructure may be favorable for NSCs to absorb nutrients, ECM proteins, and growth factors. NSCs grown on PHBHHx nanofiber matrices expressed higher levels of neuronal marker β-III tubulin than those on PHA nanofiber matrices, except for PHBHHx or PHA films.[227] NSCs on PHBHHx nanofiber matrices appeared to be more suitable for NSC attachment, synaptic outgrowth, and synaptogenesis than other PHA nanofibers and films.[227]

Collagen type I in native tissue consists of three collagen polypeptide chains that form a ropelike superhelix conformation and assemble into nanofibers ranging in size from 50 to 500 nm.[225,229] However, typical collagen 3-D scaffolds do not appear to be composed of nanofiber networks, but rather generated hydrogels or porous sponges. There are only a few reported collagen nanofiber matrices in the literature that are prepared with the phase separation method for stem cell culture and differentiation.[230]

Orza et al. prepared gold-coated collagen nanofiber matrices by a single-step reduction process using collagen solution, a reduction agent (sodium citrate or sodium borohydrate), and $HAuCl_4$.[230] These matrices were electrically conductive due to their gold coating and had fiber widths of 20−65 nm depending on the preparation conditions. Gold-coated collagen fibers seem to maintain their native ropelike superhelix conformation and their nanofiber assemblies. It was determined that placental-derived MSCs experienced accelerated neural differentiation and developed more characteristic neural lineage morphologic features when they were cultured on gold-coated nanofiber matrices in neural differentiation medium.[230] MSCs grown on the gold-coated nanofiber matrices responded within 1−2 days to neuronal induction medium by generating cells bearing neuronal-like extensions and more neuronal-like morphologies compared with the cells cultivated on conventional control culture dishes.[230] Twenty-four hours of electrical stimulation with a neuronal differentiation protocol further accelerated the acquisition of neural morphology, and after 2 days, MSCs were largely oriented in the same direction.[230] Transmitting electrical stimulation to the MSCs was effective due to the electrically conductive properties of the gold-coated nanofiber matrices.

The gold-coated nanofiber matrices were also able to induce MSCs to differentiate into myocardiocytes efficiently when cultured in myocardiocyte induction media.[230] MSCs on gold-coated nanofiber matrices were strongly positive for the cardiac marker atrial natriuretic peptide (ANP), a cardiac hormone, and early cardiac-specific homeobox protein (Nkx2.5), in contrast to MSCs on conventional control culture dishes.[230]

The phase inversion method allows for the simple preparation of nanofiber matrices compared with the methods of peptide amphiphile self-assembly and electrospinning. However, it is difficult for cells to migrate into the inside of the nanofiber matrices prepared by the phase separation method, causing cells to generally remain on the surface. Therefore, due to the difficulty of 3-D culture on nanofiber matrices prepared by the phase separation method, stem cell culture and differentiation on nanofiber scaffolds prepared by peptide amphiphile self-assembly or electrospinning seem to be more useful than those prepared by the phase separation method for clinical applications. However, scaffolds with micropores prepared by the phase separation method, such as microporous sponges, are frequently used in tissue engineering and regenerative medicine for the immobilization and entrapment of stem cells.

4. CONCLUSION

The regulation of stem cell differentiation into specific lineages remains unclear. Cell culture materials should be developed with physical, biochemical, and biomechanical cues for this purpose. The development of biomaterials requires a multidisciplinary approach, combining the selection of specific ECM proteins, appropriately ordered scaffold structures, adequate elasticity, appropriate biomaterial morphology, and appropriate biomechanical stimulation, and it will open the door to the guided differentiation of stem cells into specific lineages. It is challenging to regulate stem cell differentiation fate by regulating their microenvironment, such as by controlling only physical matrix or substrate parameters in the stem cell niche, because biological cues can effectively decide stem cell fate. However, this topic also has a deep meaning in terms of human society; our ability and performance can be improved by our (micro)environment, which is not decided solely by heredity. We believe that the role of the stem cell microenvironment in guiding and deciding stem cell differentiation fate is similar to the fate of humans in our society.

AUTHOR INFORMATION

Corresponding Author

*Tel: +866-34227151-34253. Fax: +866-3-2804271. E-mail: higuchi@ncu.edu.tw.

Notes

The authors declare no competing financial interest.

Biographies

Akon Higuchi is a Chair (Distinguished) Professor in Department of Chemical and Materials Engineering, National Central University. He was also joined to Department of Reproduction, National Research Institute for Child Health and Development, and Cathay Medical Research Institute, Cathay General Hospital, as a special researcher. He received his B.S. in Tokyo Institute of Technology in 1979 and his Ph.D. in Tokyo Institute of Technology in 1985. He was a Professor in Department of Materials & Life Science in Seikei University from 1993 to 2007. He received Sofue Memorial Award from Society of Fiber Science, Japan, in 1994 and Seikei Academic Award from Seikei Alumni Association in 2003. He is interesting in the development of materials for stem cell research. He established purification methods of hematopoietic stem cells and mesenchymal stem cells from umbilical

cord blood and adipose tissue, respectively, by a filtration method through polymeric porous membranes. He is also developing culture materials for stem cells.

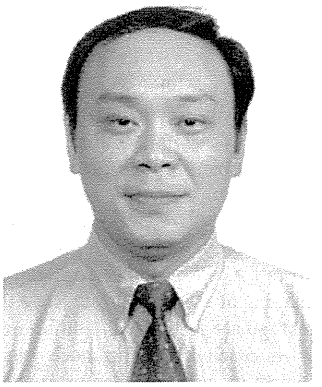

Qing-Dong Ling is a Senior Scientist and the vice minister of the Department of Medical Reserch, Cathay General Hospital, in Taipei, Taiwan. In 2006, he was joined to the Graduate Institute of Systems Biology and Bioinformatics, the National Central University, as an adjunct associate professor. He received his B.S. and DDS Degrees in Medical School, Zhejiang University, in 1979 and Ph.D. Degree in Dental Medicine from Tokyo Dental College in 1996. He spent two and half years at the National Institutes of Health as a visiting fellow from 1996 to 1999. Dr. Ling's research interests include cellular and molecular mechanisms in neuronal plasticity following neonatal inflammation, gene expression in cancer and stem cells using microarray experiments, and signal transduction and systems biology of stem cells.

Yung Chang was born in March 7, 1976, in Tokyo, Japan. He received a B.E. degree from Chung Yuan Christian University in 1998 and a Ph.D. from National Taiwan University in 2004. He was a postdoctoral fellow in Prof. Shaoyi Jiang's group at University of Washington from 2004 to 2006. He joined the Department of Chemical Engineering of Chung Yuan Christian University in 2006 and is currently an Associate Professor. In 2012, he received a NSC Wu Da-Yu Award for outstanding young scientist from National Science Council in Taiwan. He is developing a new generation of nonfouling biomaterials, which are very useful as antifouling coating agents, membrane bioseparation, hemocompatible biomaterials, tissue engineering scaffolds, drug-delivery carriers, and blood-cell filters, due to their super-biocompatibility.

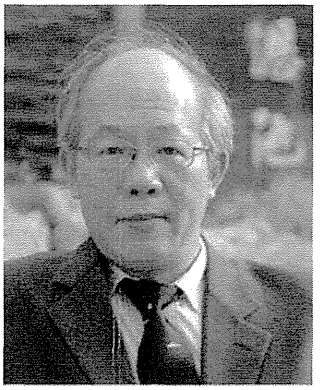

Shih-Tien Hsu was born on December 17, 1955, in Taipei, Taiwan. He received a M.D. degree from China Medical University in 1982 and a M.P.H. from Harvard School of Public Health in 1993. He received residency training in the Department of Internal Medicine in Chang-Gung Memorial Hospital from 1984 to 1987. Then, he joined the Taipei Hospital of Department of Health since 1987. Later, he completed the fellowship training of Department of Pulmonary Medicine and Critical Medicine in National Taiwan University Hospital in 1989. His research and interests were in the fields of Pulmonary Medicine, Geriatric Medicine, and Occupational Medicine, and Community Medicine. He has been to Tokyo University and Michigan University Hospital for study. He joined the Landseed Hospital in 1998 and is currently the Vice-President of Landseed Hospital. Also, he is currently CIO of Landseed Medical Internal Group.

Akihiro Umezawa is a Department Head and Chairman in Department of Reproductive Biology at National Research Institute for Child Health and Development. He received his M.D. at Keio University School of Medicine in 1985 and his Ph.D. at Keio University Graduate School of Medicine in 1990. He served as an Associate Professor in Department of Pathology at Keio University School of Medicine until 2002. He also served as an adjunct Professor at Keio University and Seikei University. He received Henry Christian Memorial Award from American Federation for Clinical Research Foundation in 1993 and Kitasato Award from School of Medicine at Keio University in 1997. Dr. Umezawa's research focuses on stem cell-based therapy using induced pluripotent stem cells, embryonic stem cells, and mesenchymal stem cells.

ACKNOWLEDGMENTS

This research was partially supported by the National Science Council of Taiwan under Grant Nos. NSC100-2120-M-008-004 and NSC101-2120-M-008-003. This work was also

supported by the Cathay General Hospital Project (Grants 100CGH-NCU-B1 and 101CGH-NCU-A2) and the LandSeed Hospital Project (Grants 100LSH-NCU-7 and NCU-LSH-101-A-001). Grants-in-Aid for Scientific Research (No. 24560968) from the Ministry of Education, Culture, Sports, Science, and Technology of Japan are also acknowledged.

REFERENCES

(1) Osakada, F.; Ikeda, H.; Mandai, M.; Wataya, T.; Watanabe, K.; Yoshimura, N.; Akaike, A.; Sasai, Y.; Takahashi, M. *Nat. Biotechnol.* **2008**, *26*, 215.
(2) Higuchi, A.; Ling, Q. D.; Ko, Y. A.; Chang, Y.; Umezawa, A. *Chem. Rev.* **2011**, *111*, 3021.
(3) Higuchi, A.; Ling, Q. D.; Hsu, S. T.; Umezawa, A. *Chem. Rev.* **2012**, *112*, 4507.
(4) Thomson, J. A.; Itskovitz-Eldor, J.; Shapiro, S. S.; Waknitz, M. A.; Swiergiel, J. J.; Marshall, V. S.; Jones, J. M. *Science* **1998**, *282*, 1145.
(5) Reubinoff, B. E.; Pera, M. F.; Fong, C. Y.; Trounson, A.; Bongso, A. *Nat. Biotechnol.* **2000**, *18*, 399.
(6) Judson, R. L.; Babiarz, J. E.; Venere, M.; Blelloch, R. *Nat. Biotechnol.* **2009**, *27*, 459.
(7) Lutolf, M. P.; Gilbert, P. M.; Blau, H. M. *Nature* **2009**, *462*, 433.
(8) Takahashi, K.; Yamanaka, S. *Cell* **2006**, *126*, 663.
(9) Okita, K.; Ichisaka, T.; Yamanaka, S. *Nature* **2007**, *448*, 313.
(10) Yu, J. Y.; Vodyanik, M. A.; Smuga-Otto, K.; Antosiewicz-Bourget, J.; Frane, J. L.; Tian, S.; Nie, J.; Jonsdottir, G. A.; Ruotti, V.; Stewart, R.; Slukvin, I. I.; Thomson, J. A. *Science* **2007**, *318*, 1917.
(11) Lin, S. L.; Chang, D. C.; Chang-Lin, S.; Lin, C. H.; Wu, D. T.; Chen, D. T.; Ying, S. Y. *RNA* **2008**, *14*, 2115.
(12) Zhou, H.; Wu, S.; Joo, J. Y.; Zhu, S.; Han, D. W.; Lin, T.; Trauger, S.; Bien, G.; Yao, S.; Zhu, Y.; Siuzdak, G.; Scholer, H. R.; Duan, L.; Ding, S. *Cell Stem Cell* **2009**, *4*, 381.
(13) Caiazzo, M.; Dell'Anno, M. T.; Dvoretskova, E.; Lazarevic, D.; Taverna, S.; Leo, D.; Sotnikova, T. D.; Menegon, A.; Roncaglia, P.; Colciago, G.; Russo, G.; Carninci, P.; Pezzoli, G.; Gainetdinov, R. R.; Gustincich, S.; Dityatev, A.; Broccoli, V. *Nature* **2011**, *476*, 224.
(14) Nakagawa, M.; Koyanagi, M.; Tanabe, K.; Takahashi, K.; Ichisaka, T.; Aoi, T.; Okita, K.; Mochiduki, Y.; Takizawa, N.; Yamanaka, S. *Nat. Biotechnol.* **2008**, *26*, 101.
(15) Xu, C.; Inokuma, M. S.; Denham, J.; Golds, K.; Kundu, P.; Gold, J. D.; Carpenter, M. K. *Nat. Biotechnol.* **2001**, *19*, 971.
(16) Witkowska-Zimny, M.; Walenko, K.; Walkiewicz, A. E.; Pojda, Z.; Przybylski, J.; Lewandowska-Szumiel, M. *Acta Biochim. Pol.* **2012**, *59*, 261.
(17) Wu, C. H.; Lee, F. K.; Suresh Kumar, S.; Ling, Q. D.; Chang, Y.; Wang, H. C.; Chen, H.; Chen, D. C.; Hsu, S. T.; Higuchi, A. *Biomaterials* **2012**, *33*, 8228.
(18) Higuchi, A.; Shen, P. Y.; Zhao, J. K.; Chen, C. W.; Ling, Q. D.; Chen, H.; Wang, H. C.; Bing, J. T.; Hsu, S. T. *Tissue Eng., Part A* **2011**, *17*, 2593.
(19) Huebsch, N.; Arany, P. R.; Mao, A. S.; Shvartsman, D.; Ali, O. A.; Bencherif, S. A.; Rivera-Feliciano, J.; Mooney, D. J. *Nat. Mater.* **2010**, *9*, 518.
(20) Benoit, D. S.; Schwartz, M. P.; Durney, A. R.; Anseth, K. S. *Nat. Mater.* **2008**, *7*, 816.
(21) Zemel, A.; Rehfeldt, F.; Brown, A. E.; Discher, D. E.; Safran, S. A. *Nat. Phys.* **2010**, *6*, 468.
(22) Trappmann, B.; Gautrot, J. E.; Connelly, J. T.; Strange, D. G. T.; Li, Y.; Oyen, M. L.; Stuart, M. A. C.; Boehm, H.; Li, B. J.; Vogel, V.; Spatz, J. P.; Watt, F. M.; Huck, W. T. S. *Nat. Mater.* **2012**, *11*, 642.
(23) Estes, B. T.; Diekman, B. O.; Gimble, J. M.; Guilak, F. *Nat. Protoc.* **2010**, *5*, 1294.
(24) Tran, T. T.; Kahn, C. R. *Nat. Rev. Endocrinol.* **2010**, *6*, 195.
(25) Bonab, M. M.; Alimoghaddam, K.; Talebian, F.; Ghaffari, S. H.; Ghavamzadeh, A.; Nikbin, B. *BMC Cell Biol.* **2006**, *7*, No. 14.
(26) Madeira, A.; da Silva, C. L.; dos Santos, F.; Camafeita, E.; Cabral, J. M. S.; Sa-Correia, I. *PLoS One* **2012**, *7*, No. e43523.
(27) Zhao, Y. M.; Waldman, S. D.; Flynn, L. E. *Cells Tissues Organs* **2012**, *195*, 414.
(28) Gruber, H. E.; Somayaji, S.; Riley, F.; Hoelscher, G. L.; Norton, H. J.; Ingram, J.; Hanley, E. N. *Biotech. Histochem.* **2012**, *87*, 303.
(29) Wilson, A.; Trumpp, A. *Nat. Rev. Immunol.* **2006**, *6*, 93.
(30) Pittenger, M. F.; Mackay, A. M.; Beck, S. C.; Jaiswal, R. K.; Douglas, R.; Mosca, J. D.; Moorman, M. A.; Simonetti, D. W.; Craig, S.; Marshak, D. R. *Science* **1999**, *284*, 143.
(31) Alberti, K.; Davey, R. E.; Onishi, K.; George, S.; Salchert, K.; Seib, F. P.; Bornhauser, M.; Pompe, T.; Nagy, A.; Werner, C.; Zandstra, P. W. *Nat. Methods* **2008**, *5*, 645.
(32) Engler, A. J.; Sen, S.; Sweeney, H. L.; Discher, D. E. *Cell* **2006**, *126*, 677.
(33) Lee, D. A.; Knight, M. M.; Campbell, J. J.; Bader, D. L. *J. Cell. Biochem.* **2011**, *112*, 1.
(34) Chen, W. Q.; Villa-Diaz, L. G.; Sun, Y. B.; Weng, S. N.; Kim, J. K.; Lam, R. H. W.; Han, L.; Fan, R.; Krebsbach, P. H.; Fu, J. P. *ACS Nano* **2012**, *6*, 4094.
(35) Kasten, A.; Muller, P.; Bulnheim, U.; Groll, J.; Bruellhoff, K.; Beck, U.; Steinhoff, G.; Moller, M.; Rychly, J. *J. Cell. Biochem.* **2010**, *111*, 1586.
(36) Guilak, F.; Cohen, D. M.; Estes, B. T.; Gimble, J. M.; Liedtke, W.; Chen, C. S. *Cell Stem Cell* **2009**, *5*, 17.
(37) Park, J. S.; Huang, N. F.; Kurpinski, K. T.; Patel, S.; Hsu, S.; Li, S. *Front. Biosci.* **2007**, *12*, 5098.
(38) Li, D.; Zhou, J. X.; Chowdhury, F.; Cheng, J. J.; Wang, N.; Wang, F. *Regener. Med.* **2011**, *6*, 229.
(39) Falconnet, D.; Csucs, G.; Grandin, H. M.; Textor, M. *Biomaterials* **2006**, *27*, 3044.
(40) Wescoe, K. E.; Schugar, R. C.; Chu, C. R.; Deasy, B. M. *Cell Biochem. Biophys.* **2008**, *52*, 85.
(41) Burdick, J. A.; Vunjak-Novakovic, G. *Tissue Eng., Part A* **2009**, *15*, 205.
(42) Huang, N. F.; Lee, R. J.; Li, S. *Tissue Eng.* **2007**, *13*, 1809.
(43) Clause, K. C.; Liu, L. J.; Tobita, K. *Cell Commun. Adhes.* **2010**, *17*, 48.
(44) Titushkin, I.; Sun, S.; Shin, J.; Cho, M. *J. Biomed. Biotechnol.* **2010**, No. 743476.
(45) Lee, K. Y.; Mooney, D. J. *Chem. Rev.* **2001**, *101*, 1869.
(46) Little, L.; Healy, K. E.; Schaffer, D. *Chem. Rev.* **2008**, *108*, 1787.
(47) Dellatore, S. M.; Garcia, A. S.; Miller, W. M. *Curr. Opin. Biotechnol.* **2008**, *19*, 534.
(48) Boskey, A. L.; Roy, R. *Chem. Rev.* **2008**, *108*, 4716.
(49) Mei, Y.; Saha, K.; Bogatyrev, S. R.; Yang, J.; Hook, A. L.; Kalcioglu, Z. I.; Cho, S. W.; Mitalipova, M.; Pyzocha, N.; Rojas, F.; Van Vliet, K. J.; Davies, M. C.; Alexander, M. R.; Langer, R.; Jaenisch, R.; Anderson, D. G. *Nat. Mater.* **2010**, *9*, 768.
(50) Melkoumian, Z.; Weber, J. L.; Weber, D. M.; Fadeev, A. G.; Zhou, Y.; Dolley-Sonneville, P.; Yang, J.; Qiu, L.; Priest, C. A.; Shogbon, C.; Martin, A. W.; Nelson, J.; West, P.; Beltzer, J. P.; Pal, S.; Brandenberger, R. *Nat. Biotechnol.* **2010**, *28*, 606.
(51) Gilbert, P. M.; Havenstrite, K. L.; Magnusson, K. E.; Sacco, A.; Leonardi, N. A.; Kraft, P.; Nguyen, N. K.; Thrun, S.; Lutolf, M. P.; Blau, H. M. *Science* **2010**, *329*, 1078.
(52) Ghafar-Zadeh, E.; Waldeisen, J. R.; Lee, L. P. *Lab Chip* **2011**, *11*, 3031.
(53) Balakrishnan, B.; Banerjee, R. *Chem. Rev.* **2011**, *111*, 4453.
(54) Kim, B. S.; Park, I. K.; Hoshiba, T.; Jiang, H. L.; Choi, Y. J.; Akaike, T.; Cho, C. S. *Prog. Polym. Sci.* **2011**, *36*, 238.
(55) Liao, S.; Chan, C. K.; Ramakrishna, S. *Mater. Sci. Eng., C* **2008**, *28*, 1189.
(56) Kshitiz; Park, J.; Kim, P.; Helen, W.; Engler, A. J.; Levchenko, A.; Kim, D. H. *Integr. Biol.* **2012**, *4*, 1008.
(57) Discher, D. E.; Mooney, D. J.; Zandstra, P. W. *Science* **2009**, *324*, 1673.
(58) Evans, N. D.; Minelli, C.; Gentleman, E.; LaPointe, V.; Patankar, S. N.; Kallivretaki, M.; Chen, X. Y.; Roberts, C. J.; Stevens, M. M. *Eur. Cells Mater.* **2009**, *18*, 1.
(59) Pek, Y. S.; Wan, A. C. A.; Ying, J. Y. *Biomaterials* **2010**, *31*, 385.

(60) Yim, E. K. F.; Darling, E. M.; Kulangara, K.; Guilak, F.; Leong, K. W. *Biomaterials* **2010**, *31*, 1299.
(61) Luo, X. J.; Chen, J.; Song, W. X.; Tang, N.; Luo, J. Y.; Deng, Z. L.; Sharff, K. A.; He, G.; Bi, Y.; He, B. C.; Bennett, E.; Huang, J. Y.; Kang, Q.; Jiang, W.; Su, Y. X.; Zhu, G. H.; Yin, H.; He, Y.; Wang, Y.; Souris, J. S.; Chen, L.; Zuo, G. W.; Montag, A. G.; Reid, R. R.; Haydon, R. C.; Luu, H. H.; He, T. C. *Lab. Invest.* **2008**, *88*, 1264.
(62) Saha, K.; Keung, A. J.; Irwin, E. F.; Li, Y.; Little, L.; Schaffer, D. V.; Healy, K. E. *Biophys. J.* **2008**, *95*, 4426.
(63) Murphy, C. M.; Matsiko, A.; Haugh, M. G.; Gleeson, J. P.; O'Brien, F. J. *J. Mech. Behav. Biomed.* **2012**, *11*, 53.
(64) Toh, W. S.; Lim, T. C.; Kurisawa, M.; Spector, M. *Biomaterials* **2012**, *33*, 3835.
(65) Lozoya, O. A.; Wauthier, E.; Turner, R. A.; Barbier, C.; Prestwich, G. D.; Guilak, F.; Superfine, R.; Lubkin, S. R.; Reid, L. M. *Biomaterials* **2011**, *32*, 7389.
(66) Lanniel, M.; Huq, E.; Allen, S.; Buttery, L.; Williams, P. M.; Alexander, M. R. *Soft Matter* **2011**, *7*, 6501.
(67) Gao, L.; McBeath, R.; Chen, C. S. *Stem Cells* **2010**, *28*, 564.
(68) Xie, J. W.; Willerth, S. M.; Li, X. R.; Macewan, M. R.; Rader, A.; Sakiyama-Elbert, S. E.; Xia, Y. N. *Biomaterials* **2009**, *30*, 354.
(69) Dang, J. M.; Leong, K. W. *Adv. Mater.* **2007**, *19*, 2775.
(70) Wingate, K.; Bonani, W.; Tan, Y.; Bryant, S. J.; Tan, W. *Acta Biomater.* **2012**, *8*, 1440.
(71) Jiang, X.; Cao, H. Q.; Shi, L. Y.; Ng, S. Y.; Stanton, L. W.; Chew, S. Y. *Acta Biomater.* **2012**, *8*, 1290.
(72) Du, J.; Chen, X.; Liang, X.; Zhang, G.; Xu, J.; He, L.; Zhan, Q.; Feng, X. Q.; Chien, S.; Yang, C. *Proc. Natl. Acad. Sci. U.S.A.* **2011**, *108*, 9466.
(73) Wang, L. S.; Boulaire, J.; Chan, P. P. Y.; Chung, J. E.; Kurisawa, M. *Biomaterials* **2010**, *31*, 8608.
(74) Shih, Y. R. V.; Tseng, K. F.; Lai, H. Y.; Lin, C. H.; Lee, O. K. *J. Bone Miner. Res.* **2011**, *26*, 730.
(75) Park, J. S.; Chu, J. S.; Tsou, A. D.; Diop, R.; Tang, Z. Y.; Wang, A. J.; Li, S. *Biomaterials* **2011**, *32*, 3921.
(76) Bakhru, S.; Nain, A. S.; Highley, C.; Wang, J.; Campbell, P.; Amon, C.; Zappe, S. *Integr. Biol.* **2011**, *3*, 1207.
(77) Banerjee, A.; Arha, M.; Choudhary, S.; Ashton, R. S.; Bhatia, S. R.; Schaffer, D. V.; Kane, R. S. *Biomaterials* **2009**, *30*, 4695.
(78) Kobayashi, D.; Takita, H.; Mizuno, M.; Totsuka, Y.; Kuboki, Y. *J. Biochem.* **1996**, *119*, 475.
(79) Kilian, K. A.; Bugarija, B.; Lahn, B. T.; Mrksich, M. *Proc. Natl. Acad. Sci. U.S.A.* **2010**, *107*, 4872.
(80) Xu, J.; Wang, W.; Ludeman, M.; Cheng, K.; Hayami, T.; Lotz, J. C.; Kapila, S. *Tissue Eng., Part A* **2008**, *14*, 667.
(81) Qian, S. W.; Li, X.; Zhang, Y. Y.; Huang, H. Y.; Liu, Y.; Sun, X.; Tang, Q. Q. *BMC Dev. Biol.* **2010**, *10*, No. 47.
(82) Lecina, M.; Ting, S.; Choo, A.; Reuveny, S.; Oh, S. *Tissue Eng., Part C* **2010**, *16*, 1609.
(83) van Dijk, A.; Niessen, H. W. M.; Doulabi, B. Z.; Visser, F. C.; van Milligen, F. *J. Cell Tissue Res.* **2008**, *334*, 457.
(84) Mooney, E.; Mackle, J. N.; Blond, D. J.; O'Cearbhaill, E.; Shaw, G.; Blau, W. J.; Barry, F. P.; Barron, V.; Murphy, J. M. *Biomaterials* **2012**, *33*, 6132.
(85) Wang, P. Y.; Tsai, W. B.; Voelcker, N. H. *Acta Biomater.* **2012**, *8*, 519.
(86) Semenov, O. V.; Malek, A.; Bittermann, A. G.; Voros, J.; Zisch, A. H. *Tissue Eng., Part A* **2009**, *15*, 2977.
(87) Winer, J. P.; Janmey, P. A.; McCormick, M. E.; Funaki, M. *Tissue Eng., Part A* **2009**, *15*, 147.
(88) Rowlands, A. S.; George, P. A.; Cooper-White, J. J. *Am. J. Physiol.* **2008**, *295*, C1037.
(89) Chowdhury, F.; Na, S.; Li, D.; Poh, Y. C.; Tanaka, T. S.; Wang, F.; Wang, N. *Nat. Mater.* **2010**, *9*, 82.
(90) Lee, S.; Kim, J.; Park, T. J.; Shin, Y.; Lee, S. Y.; Han, Y. M.; Kang, S.; Park, H. S. *Biomaterials* **2011**, *32*, 8816.
(91) Robert, D.; Fayol, D.; Le Visage, C.; Frasca, G.; Brule, S.; Menager, C.; Gazeau, F.; Letourneur, D.; Wilhelm, C. *Biomaterials* **2010**, *31*, 1586.
(92) Li, L.; Davidovich, A. E.; Schloss, J. M.; Chippada, U.; Schloss, R. R.; Langrana, N. A.; Yarmush, M. L. *Biomaterials* **2011**, *32*, 4489.
(93) Tse, J. R.; Engler, A. J. *PLoS One* **2011**, *6*, No. e15978.
(94) Chowdhury, F.; Li, Y. Z.; Poh, Y. C.; Yokohama-Tamaki, T.; Wang, N.; Tanaka, T. S. *PLoS One* **2010**, *5*, No. e15655.
(95) McBeath, R.; Pirone, D. M.; Nelson, C. M.; Bhadriraju, K.; Chen, C. S. *Dev. Cell* **2004**, *6*, 483.
(96) Li, D.; Zhou, J. X.; Wang, L.; Shin, M. E.; Su, P.; Lei, X. H.; Kuang, H. B.; Guo, W. X.; Yang, H.; Cheng, L. Z.; Tanaka, T. S.; Leckband, D. E.; Reynolds, A. B.; Duan, E. K.; Wang, F. *J. Cell Biol.* **2010**, *191*, 631.
(97) Yang, M. T.; Fu, J. P.; Wang, Y. K.; Desai, R. A.; Chen, C. S. *Nat. Protoc.* **2011**, *6*, 187.
(98) Rehfeldt, F.; Brown, A. E. X.; Raab, M.; Cai, S. S.; Zajac, A. L.; Zemel, A.; Discher, D. E. *Integr. Biol.* **2012**, *4*, 422.
(99) Colley, H. E.; Mishra, G.; Scutt, A. M.; McArthur, S. L. *Plasma Process Polym.* **2009**, *6*, 831.
(100) Jones, R. R.; Hamley, I. W.; Connon, C. J. *Stem Cell Res.* **2012**, *8*, 403.
(101) Takahashi, Y.; Yamamoto, M.; Tabata, Y. *Biomaterials* **2005**, *26*, 3587.
(102) Zoldan, J.; Karagiannis, E. D.; Lee, C. Y.; Anderson, D. G.; Langer, R.; Levenberg, S. *Biomaterials* **2011**, *32*, 9612.
(103) Seib, F. P.; Prewitz, M.; Werner, C.; Bornhauser, M. *Biochem. Biophys. Res. Commun.* **2009**, *389*, 663.
(104) Blin, G.; Lablack, N.; Louis-Tisserand, M.; Nicolas, C.; Picart, C.; Puceat, M. *Biomaterials* **2010**, *31*, 1742.
(105) Sun, Y.; Villa-Diaz, L. G.; Lam, R. H.; Chen, W.; Krebsbach, P. H.; Fu, J. *PLoS One* **2012**, *7*, e37178.
(106) Nam, J.; Johnson, J.; Lannutti, J. J.; Agarwal, S. *Acta Biomater.* **2011**, *7*, 1516.
(107) Forte, G.; Carotenuto, F.; Pagliari, F.; Pagliari, S.; Cossa, P.; Fiaccavento, R.; Ahluwalia, A.; Vozzi, G.; Vinci, B.; Serafino, A.; Rinaldi, A.; Traversa, E.; Carosella, L.; Minieri, M.; Di Nardo, P. *Stem Cells* **2008**, *26*, 2093.
(108) Leipzig, N. D.; Shoichet, M. S. *Biomaterials* **2009**, *30*, 6867.
(109) Zhang, X.; Jaramillo, M.; Singh, S.; Kumta, P.; Banerjee, I. *PLoS One* **2012**, *7*, No. e35700.
(110) Nisbet, D. R.; Moses, D.; Gengenbach, T. R.; Forsythe, J. S.; Finkelstein, D. I.; Horne, M. K. *J. Biomed. Mater. Res., Part A* **2009**, *89A*, 24.
(111) Marklein, R. A.; Burdick, J. A. *Soft Matter.* **2010**, *6*, 136.
(112) Wang, L. S.; Du, C.; Chung, J. E.; Kurisawa, M. *Acta Biomater.* **2012**, *8*, 1826.
(113) Gonzalez-Garcia, C.; Moratal, D.; Oreffo, R. O.; Dalby, M. J.; Salmeron-Sanchez, M. *Integr. Biol.* **2012**, *4*, 531.
(114) Gobaa, S.; Hoehnel, S.; Roccio, M.; Negro, A.; Kobel, S.; Lutolf, M. P. *Nat. Methods* **2011**, *8*, 949.
(115) Chambers, I.; Silva, J.; Colby, D.; Nichols, J.; Nijmeijer, B.; Robertson, M.; Vrana, J.; Jones, K.; Grotewold, L.; Smith, A. *Nature* **2007**, *450*, 1230.
(116) Suzuki, A.; Raya, A.; Kawakami, Y.; Morita, M.; Matsui, T.; Nakashima, K.; Gaget, F. H.; Rodriguez-Esteban, C.; Belmonte, J. C. I. *Proc. Natl. Acad. Sci. U.S.A.* **2006**, *103*, 10294.
(117) Zalzman, M.; Falco, G.; Sharova, L. V.; Nishiyama, A.; Thomas, M.; Lee, S. L.; Stagg, C. A.; Hoang, H. G.; Yang, H. T.; Indig, F. E.; Wersto, R. P.; Ko, M. S. H. *Nature* **2010**, *464*, 858.
(118) Fu, J. P.; Wang, Y. K.; Yang, M. T.; Desai, R. A.; Yu, X. A.; Liu, Z. J.; Chen, C. S. *Nat. Methods* **2010**, *7*, 733.
(119) Tan, J. L.; Tien, J.; Pirone, D. M.; Gray, D. S.; Bhadriraju, K.; Chen, C. S. *Proc. Natl. Acad. Sci. U.S.A.* **2003**, *100*, 1484.
(120) Kurisawa, M.; Chung, J. E.; Yang, Y. Y.; Gao, S. J.; Uyama, H. *Chem. Commun.* **2005**, 4312.
(121) Nieponice, A.; Soletti, L.; Guan, J. J.; Deasy, B. M.; Huard, J.; Wagner, W. R.; Vorp, D. A. *Biomaterials* **2008**, *29*, 825.
(122) Zhang, G.; Drinnan, C. T.; Geuss, L. R.; Suggs, L. J. *Acta Biomater.* **2010**, *6*, 3395.
(123) Bou-Gharios, G.; Ponticos, M.; Rajkumar, V.; Abraham, D. *Cell Proliferation* **2004**, *37*, 207.